AN INVESTIGATION OF UNDERWATER WELDED HY-80 STEEL

Stanley Leon Renneker

AN INVESTIGATION OF UNDERWATER WELDED HY-80 STEEL

by

Stanley Leon Renneker

B.S., United States Coast Guard Academy

1969

SUBMITTED IN PARTIAL FULFILLMENT OF THE REQUIREMENTS FOR THE DEGREE OF OCEAN ENGINEER AND THE DEGREE OF MASTER OF SCIENCE IN NAVAL ARCHITECTURE AND MARINE ENGINEERING

at the

MASSACHUSETTS INSTITUTE OF TECHNOLOGY

June, 1974

AN INVESTIGATION OF UNDERWATER WELDED HY-80 STEEL

by

Stanley Leon Renneker

Submitted to the Department of Ocean Engineering on May 10, 1974, in partial fulfillment of the requirements for the degree of Ocean Engineer and the degree of Master of Science in Naval Architecture and Marine Engineering at the Massachusetts Institute of Technology, June, 1974.

ABSTRACT

The objective of this thesis was two fold; first was the desire to extend previous laboratory work and to evaluate the ability to fabricate acceptable underwater welded HY-80 steel joints, under working conditions, within the guidelines of the United States Navy governing underwater welding operations, and secondly was the desire to investigate the occurance of the hydrogen embrittlement phenomena in the underwater welded HY-80 steel joints.

A series of working dives, under working conditions, within the guidelines of the United States Navy governing underwater welding operations, were conducted by the author. These dives simulated the welded repair of a crack in an underwater body, in accordance with the Underwater Cutting and Welding Manual, Navships 0929-000-8010.

The results of the microscopic investigation, microhardness tests, and mechanical bend tests have indicated a capability to fabricate acceptable underwater welded HY-80 steel joints, under working conditions, within the guidelines of the United States Navy governing underwater welding operations, which do not suffer from the hydrogen embrittlement phenomena. This capability is found to exist for water environment temperatures of 25°C (77°F) and below, providing the water is clear and the welder-diver is able to use the multi-pass welding technique.

Further study is needed to determine the contribution of the thermal stresses, occuring during the underwater welding process, to the mechanical characteristics of the cracking of the underwater welded HY-80 steel joint. In addition, a study should be conducted to determine the possible effect on the hydrogen embrittlement phenomena, as a result of the application of a method of preheat and interpass heat to overcome the effects of the thermal stresses.

This thesis is presented in five parts in an effort to facilitate the needs of the readers. In addition to the parts explaining the experimental results, the findings of the author, and the references used by the author, are parts which provide extensive introductory background information and appendixes of detailed particulars. It is the hope of the author that this will provide completeness which will benefit the reader.

Thesis Supervisor: Professor Koichi Masubuchi
Title: Professor of Ocean Engineering

ACKNOWLEDGEMENTS

The author wishes to thank Professor Koichi Masubuchi for his advice, guidance, and sustaining encouragement throughout the course of this thesis. Also Mr. Anthony Zona, Mr. Arthur Greaber, and Mr. Joseph Cairn of M.I.T. and LCDR A.C. Esau, Commanding Officer, Naval School Diving and Salvage, Washington, D.C., and his staff for their assistance with the experimental portion of this thesis.

Finally, thank you to my wife, Barbara, for her understanding throughout the course of this thesis and her patience and diligence in typing this manuscript.

TABLE OF CONTENTS

PAGE

LIST OF FIGURES

LIST OF TABLES

PART I

INTRODUCTORY BACKGROUND INFORMATION

CHAPTER 1

HYDROGEN - METAL RELATIONSHIP

GENERAL

Hydrogen gas in contact with a metal may interact with the metal in one of three manners.

1. The hydrogen gas may condense on the metal surface forming a one to two molecule thick layer: adsorption.
2. The hydrogen gas may enter into solution within the interior of the metal: absorption or occlusion.
3. Occluded gas may diffuse through the interior of the metal.

The term "sorption" is used to refer to a duplex condition in which the hydrogen gas may be present in both the adsorbed and absorbed states.

For the hydrogen to be able to diffuse through the metal it cannot be in molecular form, but must be in atomic form. This condition is due to the fact that the tendency of hydrogen to diffuse through the metal is associated with its ability to combine with the metal and is appreciable in metals in which the soluability of the hydrogen is high.

Of the four possible types of reaction that can occur when hydrogen is in contact with metal, steel forms a true solid solution with the hydrogen. This is indicated by the facts that

1. The hydrogen soluability varies as the square-root of the pressure. (Sievert's Law)

2. The soluability increases as the temperature increases. For this reason, steel is known as an endothermic occluder.

ADSORPTION

The first process to occur when hydrogen is in contact with steel is the adsorption of a layer of the gas on the surface of the metal. The amount of hydrogen that is adsorbed by a unit surface area of the steel is proportional to the pressure at any given temperature. There are three ways in which the adsorption phenomena is usually represented:

1. Adsorption isotherm; a plot of the amount of hydrogen adsorbed versus pressure, at constant temperature.
2. Isotere; a plot of the variation of equilibrium pressure with temperature, for a given quantity of adsorbed hydrogen.
3. Isobar; a plot of the variation of the amount of gas adsorbed versus temperature, at constant pressure.

The bonding characteristics of the atoms which form the surface layer of the metal are unsaturated because of the assymetrical condition of their geometry. As a result, when the molecules of hydrogen impinge upon the surface of the metal they tend to condense, and are held in position by the unsaturated field force of the atoms which form the surface layer of the steel.

In the case of hydrogen, a diatomic gas, the adsorption forces act on the individual atoms of the hydrogen molecule. Hence as the condensing molecules of hydrogen cover the surface of the metal with an adsorption film, each of the atoms is held individually and the molecule will lose its identity. Although it is necessary for two adjacent adsorption sites on the surface of the metal to be vacant for adsorption to occur, it is a matter of statistical chance whether an evaporating molecule will contain the same two atoms which condensed as a molecule, or whether such a molecule will contain two atoms from adjacent adsorption sites, which condensed from two different molecules.

The steady-state adsorption film of hydrogen on the surface of steel is the net result of two opposing factors:

1. The condensation of hydrogen on the surface of the metal in order to saturate the bonding characteristics of the metal surface.
2. The evaporation of the gas from the surface of the metal in equilibrium with the external pressure.

In the case of some of the atoms which comprise the alloying elements of steel, the amount of hydrogen that is adsorbed on the surface of the metal decreases as the temperature increases. This type of adsorption is usually referred to as "physical adsorption".

However, in the case of some of the atoms which comprise the alloying elements of steel, the amount of hydrogen that is adsorbed on the surface of the metal is more complex. It has been observed that as the temperature increases the adsorption will decrease to a minimum value, and then increase as the temperature increases further. This rise in adsorption will continue to a maximum value and then decrease as the temperature continues to increase.

This type of adsorption is usually refered to a chemi-adsorption and is dependent upon the chemical attraction between the metal surface and the hydrogen.

Physical adsorption is a fully reversible phenomena with respect to pressure and temperature. However, chemi-adsorption is not fully reversible, particularly with respect to temperature.

ENDOTHERMIC OCCLUSION

In the periodic table, endothermic occluders (hydrogen soluability on the order of 0.1 atomic percent) all lie mid-way between the exothermic occluders (hydrogen soluability on the order of 2 to 10 atomic percent) and those elements which do not absorb hydrogen.

In the case of steel, as with all endothermic occluders, the only reaction that occurs with hydrogen is the formation of a simple

solid-solution, the soluability of which increases with temperature and is proportional to the square-root of the hydrogen pressure. The soluability of hydrogen in metal can be expressed by an equation of the form:[11]

$$S = S_o\sqrt{P} \exp(-Q/2RT) \qquad (1)$$

Where: S = Soluability of hydrogen

S_o = Constant

P = Pressure of hydrogen

Q = Heat of solution, in calories per gram-mole of hydrogen

R = Gas constant

T = Temperature in degrees Absolute

DIFFUSION

Although the mechanism of hydrogen diffusion in metals is by no means clear, it would appear that the various possibilities are that hydrogen atoms may diffuse through:

1. The interstices of the lattice structure.
2. Grain boundaries.
3. Structural imperfections within grains.

In the case of iron, interstitial diffusion is the predominant

means, although the grain-boundaries and lattice structures are of secondary importance.

A necessary preliminary though, to the diffusion of hydrogen through the metal, regardless of means, is the dissociation of the hydrogen molecule to atomic hydrogen at the adsorption surface.

Diffusivity increases rapidly with temperature in accordance with the exponantial law governing rate processes, and is proportional to the square-root of the hydrogen pressure. Figure 1-1 shows the variation of the overall hydrogen diffusivity coefficient with respect to temperature. The diffusivity of hydrogen in metal can be expressed by an equation of the form:(17)

$$D = D_o\sqrt{P}\ \exp\ (-Q/2RT) \qquad (2)$$

Where: D = Diffusivity of hydrogen

D_o = Constant

P = Pressure of hydrogen

Q = Heat of solution, in calories per gram-mole of hydrogen

R = Gas constant

T = Temperature in degrees Absolute

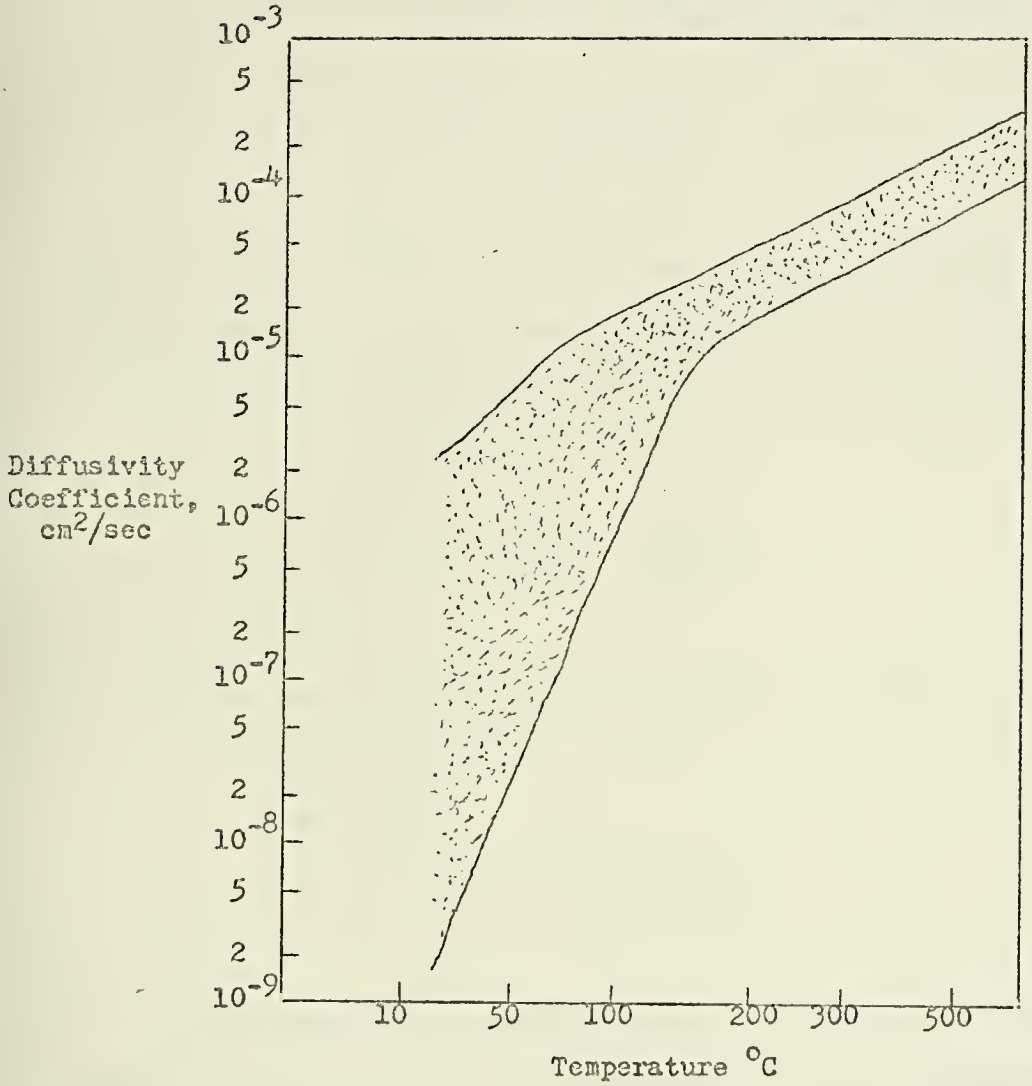

FIGURE 1-1: VARIATION OF THE OVERALL HYDROGEN DIFFUSIVITY COEFFICIENT WITH TEMPERATURE (10)

DETERMINATION OF DIFFUSIVITY COEFFECIENT AND SOLUABILITY LIMIT

Two ways of determining the diffusivity coefficient and the soluability limit are by:

1. Hydrogen evolution rate data
2. Permeation rate data.

Both of these methods are based on the microscopic dispersion of hydrogen in steel as expressed in the form of heat flow in a conductor. This expression is known as Fick's Second Law[17]:

$$\frac{\partial c}{\partial t} = D\frac{\partial^2 c}{\partial x^2} \qquad (3)$$

Where: c = Hydrogen concentration at a point

x = Distance

t = Time

D = Diffusivity coefficient

Hydrogen evolution rate data. For this method of determining the diffusivity coefficient and soluability limit an infinitely large plate is assumed, with cathodic charging from both sides.

The following boundary conditions are applied to Fick's Second Law[17]:

$$c = 0 \quad \text{at} \quad t = 0$$

$$c = C_o \quad \text{at} \quad t = \infty$$

$$c = 0 \quad \text{at} \quad x = 0, \quad t \quad 0,$$

$$c = C_o \quad \text{at} \quad x = \ell, \quad t \quad 0$$

Where: t = Time

x = Distance into plate in a normal direction

L = Thickness of the plate

C_o = Saturation concentration on the plate surface.

The solution of Fick's Second Law with these boundary conditions results in[17]:

$$Cav/C_o = 1 - \frac{4}{2} \sum_{n=1}^{\infty} \frac{1 - (-1)^n}{n^2} \exp\left[-(n\pi/\ell^2)Dt\right] \qquad (4)$$

Where: Cav/C_o = Concentration average over the plate volume

Dt/ℓ^2 = Fourier number

Figure 1-2 shows a graphical representation of the calculated results of the concentration average over the plate volume versus the Fourier number. This curve represents how the volume of occluded hydrogen changes with the charging time.

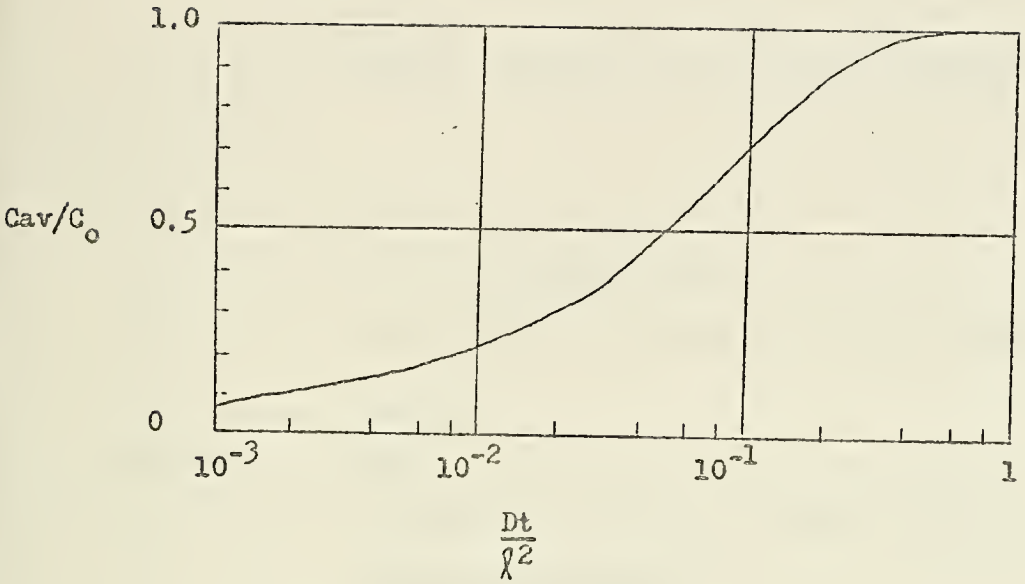

FIGURE 1-2: CALCULATED VALUES OF CONCENTRATION AVERAGE VERSUS FOURIER NUMBER OBTAINED FROM HYDROGEN EVOLUTION RATE DATA (17)

Permeation rate data: For this method of determining the diffusivity coefficient and solubility limit an infinitely large plate is assumed, with a constant cathodic charge at the surface of the plate.

The following boundary conditions are applied to Fick's Second Law[17]:

$t = 0$ at $c = 0$

$x = 0$, t 0 at $c = o$ (at the surface)

$x = \ell$, t 0 at $c = C_o$ (at the hydrogen charging surface)

Where: t = Time

x = Distance into plate in a normal direction

L = Thickness of the plate

C_o = Saturation concentration on the charging surface

The hydrogen permeation volume through a unit area of the plate after a time t of cathodic charging is expressed as[17]:

$$Z = \int_o^t D(dc/dx)_{x=0}dt =$$

$$\frac{DC_o}{l}\left\{t + 2\sum_{n=1}^{\infty}\frac{(-1)^n}{n^2} \times \frac{\ell^2}{Dn^2}\left[1-\exp(-(n/\ )^2Dt)\right]\right\} \qquad (5)$$

for the temperature range where[17]:

$$Z = \frac{DC_o}{\ell} \quad t = \frac{2\ell^2}{D^2} \sum_{n=1}^{\infty} \frac{(-1)^n}{n^2} =$$

$$\frac{DC_o}{\ell}\left[t + \frac{2\ell^2}{2^2}\left(-\frac{2}{12}\right)\right] =$$

$$\frac{DC_o}{\ell}\left[t - \frac{\ell^2}{6D}\right] \qquad (6)$$

Defining two quantities in the above expression as (17):

$$\frac{DC_o}{\ell} = P = \text{Permeation rate}$$

$$\frac{\ell^2}{6D} = L = \text{Lag-time}$$

the expression for the "Lag-Time Method" is obtained:[17]

$$Z = P(t-L) \qquad (7)$$

Figure 1-3 gives a graphical representation of this expression.

A comparison of the diffusivity coefficient and the soluability limit determined by the hydrogen evolution rate data and permeation rate data methods reveal that:

1. The diffusivity coefficient, D (cm^2/sec), evaluated by the hydrogen evolution rate data method is approximately two times greater than the one evaluated by the permeation rate data method.

2. The soluability limit, c (cc/100g Fe), evaluated by the hydrogen evolution rate data method is approximately equal to the one evaluated by the permeation rate data method.

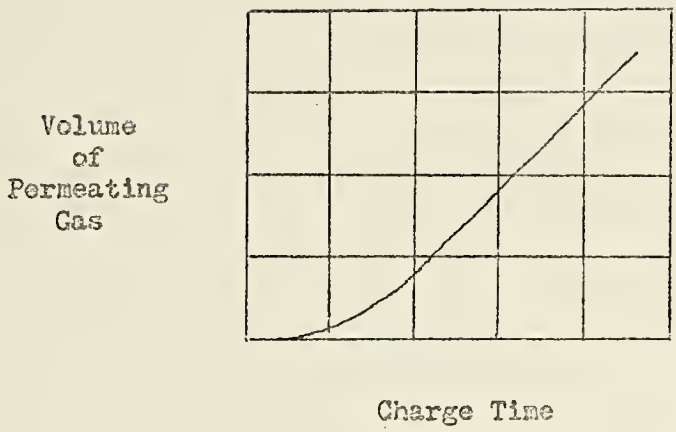

FIGURE 1-3: TIME-LAG METHOD PLOT OF VOLUME OF PERMEATING GAS VERSUS CHARGING TIME OBTAINED FROM PERMEATION RATE DATA (17)

CHAPTER 2

HYDROGEN EMBRITTLEMENT OF STEEL

GENERAL

"It is still not possible to offer a convincing explanation of precisely how the presence of hydrogen within the metal structure leads to the formation of cracks in certain circumstances and not in others."[10]

This situation exists today dispite the considerable amount of research that has been conducted on the phenomena of hydrogen-induced embrittlement in steel. There have been over 1200 references of relevant literature printed on the subject since 1926.[11]

Yet, it is possible to summarize the phenomena[11]:

"Hydrogen embrittlement occurs under those conditions of composition, temperature, and strain-rate, for which the presence of hydrogen leads to the formation and propagation of brittle micro-cracks, when such cracks would not be formed in the absence of hydrogen; when these conditions do not apply the presence of hydrogen does not lead to embrittlement."

and list a summary of the characteristics of the physical effects of hydrogen on the mechanical properties of iron and steel[11]:

1. Elastic properties are not significantly effected by the presence of hydrogen.
2. Hydrogen solution in the range of 0-10 $cm^3/100g$ Fe has no effect on the hardness although the ultimate tensile

strength is decreased.

3. The fracture stress is lowered in proportion to the increase in the hydrogen concentration.

4. At low temperatures, hydrogen can produce a small yeild point in pure iron. While at normal temperatures hydrogen can prevent the occurance of the yeild phenomena which are usually found in mild steel.

5. Both of the ductility parameters of elongation and reduction of area are reduced in proportion to the hydrogen concentration up to a value of 5 $cm^3/100g$ Fe (approximately 0.025 atomic percent). At greater concentrations of hydrogen the ductility is constant.

6. As the strain rate is increased, the hydrogen embrittlement is reduced. Thus hydrogen has virtually no effect in the limiting case of the impact test.

7. The maximum hydrogen embrittlement effect occurs at temperatures just above the ductile-to-brittle transition for the hydrogen-free material and can range from $-100^{\circ}c$ to $+100^{\circ}c$.

8. Tensile stresses are required to cause hydrogen embrittlement.

9. The presence of a hydrogen solution in steel changes the fracture type from that of a typically ductile material to that of a typically brittle material.

10. The treatment of the material governs the hydrogen embrittlement effect. Steels in a hardened or sphereodized

condition are particularly susceptible. Cold-working will also increase the susceptibility.

11. The presence of hydrogen causes "delayed failure" or "static fatigue", premature brittle fracture under static loading conditions, in high strength alloy steels.
12. Hydrogen embrittlement requires the presence of diffusible hydrogen during straining. The presence of hydrogen in steel does not affect the metal in the unstrained state and its removal prior to straining ensures full ductility.
13. The overall ductility of the metal will be typical of the locally enriched areas of hydrogen concentration, which are the least ductile, rather than the average hydrogen content.

MECHANISM OF HYDROGEN EMBRITTLEMENT

The effect of the presence of hydrogen is to produce an additional source of micro-cracks which can lead to the propagation of a brittle fracture. The presence of hydrogen within a metal will result in an embrittlement effect if its soluability and diffusivity characteristics are such as to increase the "piling-up" of dislocations, to form micro-cracks and propagate into a brittle fracture, decreasing the ability of the metal to withstand plastic deformation and thus reducing its ductility. This embrittlement occurs in steel, an endothermic occluder, as a result of an increase in the internal strain of the metal lattice because of the formation

of a tightly-packed interstitial solution of hydrogen. The mechanism is most apparent at temperatures which are just above those of the ductile-to-brittle transition of the hydrogen-free metal. Below the transition temperature, the metal is brittle regardless of the presence of hydrogen. While above the transition temperature, it is difficult for micro-cracks to form and propagate before plastic deformation takes place.

A considerable number of theories have been formulated in an effort to explain the mechanism of hydrogen embrittlement in steel. In determining the validity of the various theories the following predominant characteristics of the mechanism must be considered:

1. The reduction in ductility, resulting from the presence of hydrogen, increases as the hydrogen concentration increases to a value of 5 cm^3/g Fe. Beyond this point the ductility is uneffected by additional hydrogen content.
2. The fracture of hydrogen containing steel is essentially brittle.
3. The degree of embrittlement for a given hydrogen concentration decreases as the temperature decreases below room temperature and the strain rate increases, suggesting a diffusion controlled mechanism.
4. The degree of embrittlement for a given hydrogen concentration also decreases as the temperature rises above room temperature.

Zapffe[11] proposed a theory based on Planar pressure. The explanation stated that the hydrogen gas exerted an increased pressure on the metal lattice as more of the gas precipitated. At a critical pressure, the lattice of the metal would be sprung by the hydrostatic force of the hydrogen, at which point the steel was said to be embrittled. If at this point a stress were applied to the structure, the metal would prematurely fracture. However, the theory has several major deficiencies:

1. The absence of hydrogen embrittlement during compression.
2. The inability to account for the temperature and strain-rate relationship dependence.

Petch[11] formulated a theory based on the mechanisms of brittle fracture, which suggested that the presence of hydrogen decreased the energy necessary to form a new surface. The hydrogen atoms that are adsorbed on the surface of micro-cracks reduce the surface energy, and thereby reduce the amount of strain-energy necessary to form a new surface. This would result in the critical stress required for crack propagation to be lower in the presence of hydrogen. This theory is dependent upon the diffusion of hydrogen to the micro-cracks within the steel. It explains the dependence of hydrogen embrittlement upon the strain-rate and its decrease as the temperature falls below room temperature, but it fails to explain its decrease as the temperature rises above room temperature.

Kazinczy[11] also formulated a theory based on the mechanisms of brittle fracture. However, Kazinczy believed that the presence of hydrogen increases the energy released during crack propagation. Therefore, the energy released by the extension of the crack is greater than the energy necessary to create the new surface of the enlarged crack region, and rapid propagation and brittle fracture result. This suggests that the main factor of hydrogen embrittlement is the presence of gasious hydrogen within the micro-cracks of the steel, with the degree of embrittlement increasing as the gasious hydrogen contents increases and thus increases the pressure within the micro-crack. However, Kazinczy's theory, as was the case with Petch, is dependent upon the diffusion of hydrogen to the micro-cracks within the steel. It also explains the dependence of hydrogen embrittlement upon the strain-rate and its decrease as the temperature falls below room temperature, but it, too, fails to explain its decrease as the temperature rises above room temperature.

Vaughan and DeMorton[11] proposed a theory based on the idea of the strain-hardening effect. It is suggested that hydrogen is initially present in interstitial polution in the unstrained steel. As stresses are applied, the hydrogen diffuses to the slip planes and forms atmospheres which hinder the movement of dislocations and lead to premature brittle fracture. However, this was shown to be in direct contradiction with a corrollary hypothesis of Vaughan and DeMorton that suggests that hydrogen can suppress the yield point

phenomena, due to the hydrogen atmosphere's ability to maintain contact with the movement of dislocations, because of the high diffusion rate of hydrogen.

Rogers[11] suggests that the hydrogen atmospheres are bound less tightly to dislocations than atmospheres of carbon or nitrogen. Hydrogen would not displace a significant amount of either carbon or nitrogen from a dislocation, but would instead attach to a dislocation that had been freed of carbon and nitrogen. This hypothesis affords an explanation of the relevant behaviour of hydrogen, nitrogen, and carbon and suggests that the hydrogen embrittlement of steel is not a result of a strain-hardening mechanism.

Morlett, Johnson, and Troiano[11] have suggested a new theory based on diffused hydrogen localized at, or near to, lattice imperfections refered to as "voids". The combined effect of the diffused hydrogen and the stress system established around each "void" determine the severity of the hydrogen embrittlement effect. The "voids" are regarded as micro-notches about which a multi-axial stress system will be established when stress is applied to the steel. In a region within the metal lattice near each "void", the stress system will be tri-axial in nature. The theory suggests that it is the hydrogen concentration within the region of tri-axial stress within the metal lattice and not the hydrogen concentration

within the "void", that determines the degree of embrittlement.

During the diffusion process, hydrogen will concentrate in a highly stressed region of the lattice structure and thus create a hydrogen concentration gradient which corresponds to the multi-axial stress gradient of the region. Within this region, the hydrogen moves from the lattice into the "voids" in order to attain a state of equilibrium.

The size of the hydrogen concentration gradient that will exist in the region of tri-axial stress near a "void" will depend on:

1. The original hydrogen concentration
2. The hydrogen diffusion rate
3. The time available for the diffusion of the hydrogen.

Thus the theory essentially suggests that the stress-influenced diffusion of hydrogen results in the formation of regions of high hydrogen concentration and extreme tri-axial stress within the lattice structure of the metal. The combined effect of the hydrogen concentration and the tri-axial stress cause the initiation of a brittle micro-crack within the metal crystal. The micro-crack in turn propagates and leads to the propagation of a brittle fracture, resulting in failure of the steel.

Although the exact manner in which the concentration of hydrogen

at the region of tri-axial stress within the metal lattice, causes the initiation of a brittle micro-crack, is unexplained, and will require a further developement of the theory of fracture in metals, the theory of Morlett, Johnson, and Troiano[11] does account for the predominant characteristics of hydrogen embrittlement:

1. The decrease in the degree of hydrogen embrittlement with the decrease in temperature results from the decrease in the diffusion rate with the decrease in temperature.
2. The decrease in the degree of hydrogen embrittlement as the temperature increases results from the increase in the diffusion rate, with the resultant increase in the ease of diffusion overcoming the tendency toward stress induced concentrations of hydrogen.
3. The increase in the degree of hydrogen embrittlement as the strain-rate is decreased results from the increase in the stress-induced concentrations of hydrogen in the region of tri-axial stress within the metal lattice structure. This occurs because of the increased time of applied stress when the strain-rate is reduced, and the resultant increased influence of the tri-axial stress system upon the diffusion of the hydrogen.

Therefore, it has been stated that the theory suggested by Morlett, Johnson, and Troiano[11] presently affords the best explanation of the mechanism of the phenomena of hydrogen embrittlement in steel.

PROPAGATION OF BRITTLE FRACTURES

Once the micro-crack has been initiated by the combined effect of the hydrogen concentration and the tri-axial stress system, its propagation leading to a brittle fracture and the resultant failure of the steel is dependent upon the relative velocities of the plastic deformation and crack propagation.

Plastic flow at the point of initiation of the micro-crack should relieve the tri-axial stress concentration of the region. However, the presence of a hydrogen concentration in the region will cause a general resistance to the plastic deformation. This loss in ductility results in a retardation of the plastic flow to a rate below that of the crack velocity. The result is the propagation of the micro-crack leading to a brittle fracture and the resultant failure of the steel.

CHAPTER 3

WELD DEFECTS

GENERAL

Defects are expected to exist in a welded joint. It is not possible to completely prevent all forms of them from occuring. Therefore, it is necessary to determine the significance of the existing defects, with respect to their effect on the proper functioning of the welded joint, when it is considered in relation to the design requirements for the service life of the structure.

The significance of the existing weld defect may vary, depending upon:

1. The defects position in the weld or heat affected zone.
2. The properties of the residual stresses in the material in which the defect lies.
3. The nature of the service required.

Even the smallest of defects, on a microscopic scale, can act as an initiation point for other weld defects that could lead to a failure.

The significance of an existing weld defect, and thus the decision to accept or reject a welded joint, can be based on:

1. An arbitrary level of defects.
2. Previous experience as to the quality of weld that it is known to be possible to obtain.
3. Previous experience as to the quality of weld that it is known to be necessary in order to obtain a satisfactory

service life.

4. Scientific knowledge of the effect of defects under the relevant circumstances.

The standards that are presently being used as a basis for the "accept/reject" decision are quite arbitrary and subjective. They are not usually supported by scientific knowledge relevant to the service life of the weld joint, and, therefore, are not truely representative of the real behavior. This is pointed out by recent expermental evidence that indicates that a greater degree of tolerance as to weld defects, is possible with the new, tougher materials. However, the present standards for existing weld defects do enable manufacturers to "keep fabrication in line"(23).

POROSITY

Extreme concern exists over the less critical defect of weld metal porosity, even though a considerable degree of weld metal pososity can be tolerated.

The strength of a welded joint does not seem to be greatly effected by the size, distribution, or location of pososity within the weld metal. However, the strength does appear to decrease in proportion to the loss of the effective cross sectional area of the weld metal, as a result of the porosity.

The fatigue strength of a welded joint also seems to have a good correlation to the reduction in effective cross sectional area of the weld metal. The percentage reduction in the fatigue strength is proportional to the percentage reduction in effective cross-sectional area.

Burdekin, Harrison, and Young[7] have further stated that pores may also serve as points of stress concentration within the meld metal thus creating an internal notch effect that could cause failure during cyclic loading.

CRACKING

The temperature distribution, with time, that occurs during the process of welding a joint compares to the thermo-chemical treatment of the steel, except that the welding cycle is spontaneous and without any control of the high residual stresses and impurities. The resultant brittle fractures that occur are effected by:

1. Local volume changes.
2. Tensile stresses.
3. Local plastic deformation.
4. Hardening of the microstructure of the material.

Kovayashi and Aoshima[18] identified the cracks which occurred in low alloy steels as:

1. Underbead cracks
2. Toe cracks
3. Root cracks.

They have suggested that all of the cracks were hydrogen induced, although the tow cracks and root cracks could have also occurred without the support of induced hydrogen.

Cabelka[18] has identified four types of delayed weld cracks that were found in welded joints.

1. Underbead cracks
2. Transverse cracks
3. Notch cracks
4. Fusion cracks.

These are shown in Figure 3-1.

The underbead cracks occur below the fusion zone in the heat affected zone. For these cracks to form there must be a combination of tensile stresses, hydrogen, and a hard microstructure. Without the presence of hydrogen, underbead cracks would not occur.

Transverse cracks tend to initiate in a zone of "overheated martensite" and run perpendicular to the isotherms in the weld metal. It is possible for these cracks to run from the weld into the uneffected base metal. The transverse cracks occur as a result of shrinkage stresses, particularly when the multi-pass technique is

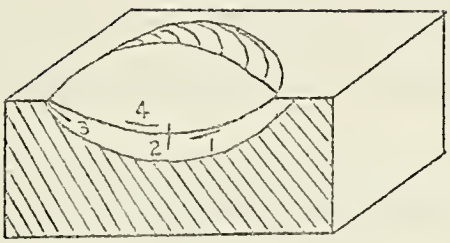

1. Underbead crack
2. Transverse crack
3. Notch crack
4. Fusion crack

FIGURE 3-1: TYPES OF DELAYED CRACKS FOUND IN WELDED JOINTS (8)

used. The presence of hydrogen only supports the initiation of the transverse cracks. It is not essential to their formation.

The initiation of fusion cracks is also not dependent upon the presence of hydrogen. However, hydrogen does support their initiation. Fusion cracks occur in the fusion zone as a result of a combination of tensile stresses and a hard microstructure.

Notch cracks occur at the toe of the weld metal and are only secondarily influenced by the presence of hydrogen.

All four types of the delayed cracks found in welded joints by Cabelka[8] tended to occur in formerly overheated regions of hard microstructure, under the influence of tensile stress components of weld metal shrinkage perpendicular to the direction of crack propagation. A phenomena similar in nature to quench cracking.

The delayed cracks were further characterized by the following:[8]

1. There is a different type of crack with regard to location and shape.
2. Each type of crack tended to retain its own specific location and direction of propagation; two or more cracks of a specific type rarely combine.
3. The formation process for each type of crack is different.
4. The difference in the crack initiation process does not occur

because of a difference in incubation periods, but because of the orientation and magnitude of the local tensile stresses.

PART II

EXPERIMENTAL RESULTS

CHAPTER 4

MICROSCOPIC INVESTIGATION

GENERAL

The specimens used for the microscopic investigation were the same as those used for the microhardness tests, and were propared as shown in Figure 5-1. Each specimen was finished on a series of finishing wheels, ranging from a #80 through #120, #240, and #320. Next, each specimen was polished on a #600 finishing wheel, using a 0.3μ alumina/distilled water solution. Finally, each specimen was etched using a 2% Nital Solution.

TEST RESULTS

The results of the microscopic investigation are shown in Figures 4-1 through 4-16. Porosity was extensive throughout the weld metal. A greater degree of porosity, and a greater number of cracks, were found in the overhead welds than in the verticle welds or the downhand welds.

The cracks which occurred were found to be in the weld metal in the form of "fusion" cracks or "transverse" cracks[8], which initiated in the weld metal and extended into the heat affected zone. Underbead cracking in the heat affected zone was not observed. This finding is in direct conflict with the findings of Masubuchi and Martin[21] and the normal occurance in air welds. However, these findings are in agreement with the findings of Meloney[22].

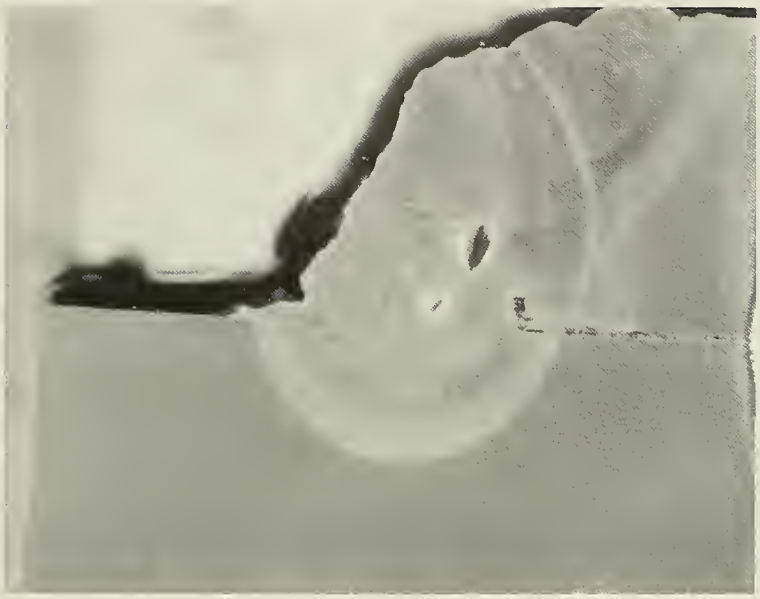

FIGURE 4-1: MULTI-PASS DOWNHAND UNDERWATER WELDED LAP JOINT #1 USING E11018 ELECTRODE (5x, 2% NITAL)

FIGURE 4-2: LAP JOINT #1 SHOWING EXTENSIVE PROOSITY THROUGHOUT WELD METAL (100x, 2% NITAL)

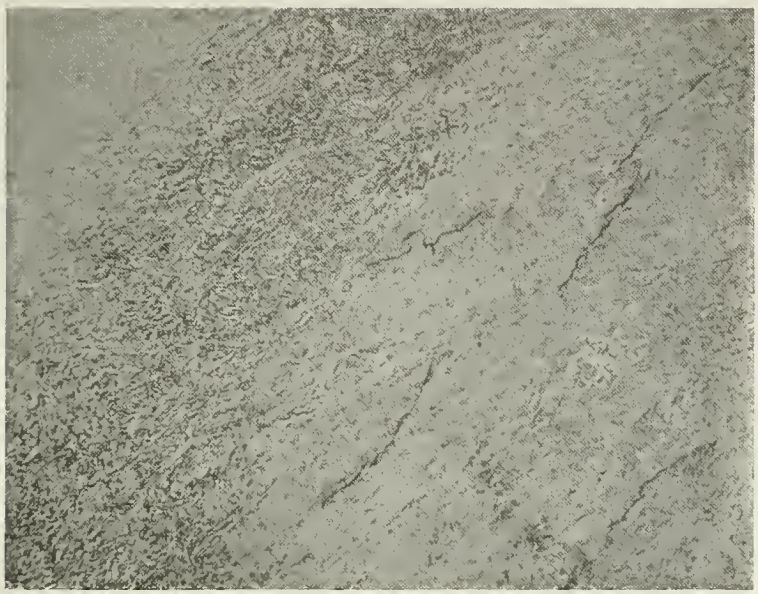

FIGURE 4-3: LAP JOINT #1 SHOWING "FUSION" CRACKS IN THE WELD METAL NEAR THE HAZ, (100x, 2% NITAL)

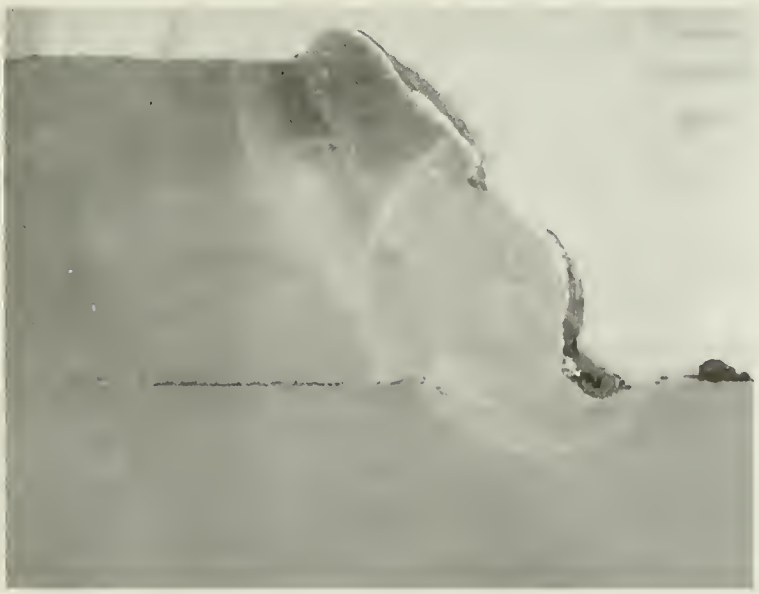

FIGURE 4-4: MULTI-PASS DOWNHAND UNDERWATER WELDED LAP JOINT #2 USING E11018 ELECTRODE (5x, 2% NITAL)

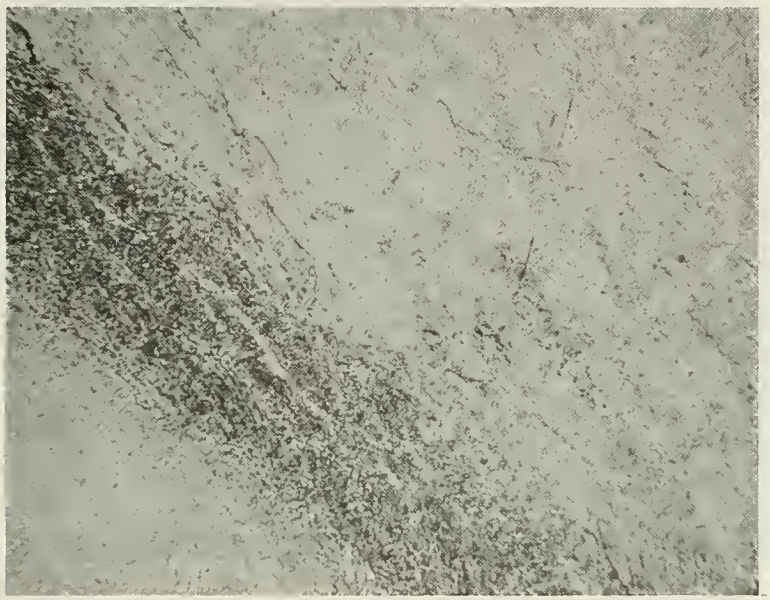

FIGURE 4-5: LAP JOINT #2 SHOWING "FUSION" CRACKS IN THE WELD METAL NEAR THE HAZ (100x, 2% NITAL)

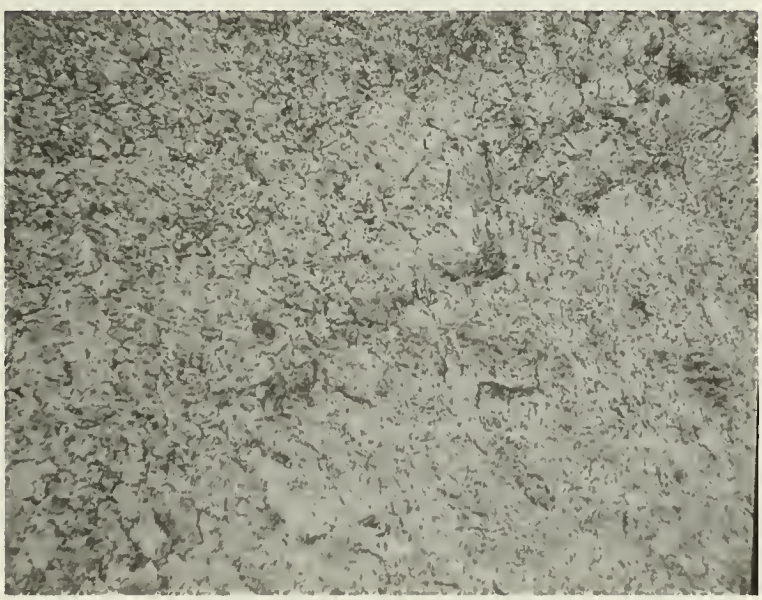

FIGURE 4-6: LAP JOINT #2 SHOWING HEAVY GRAIN BOUNDARIES IN WELD METAL NEAR HAZ (100x, 2% NITAL)

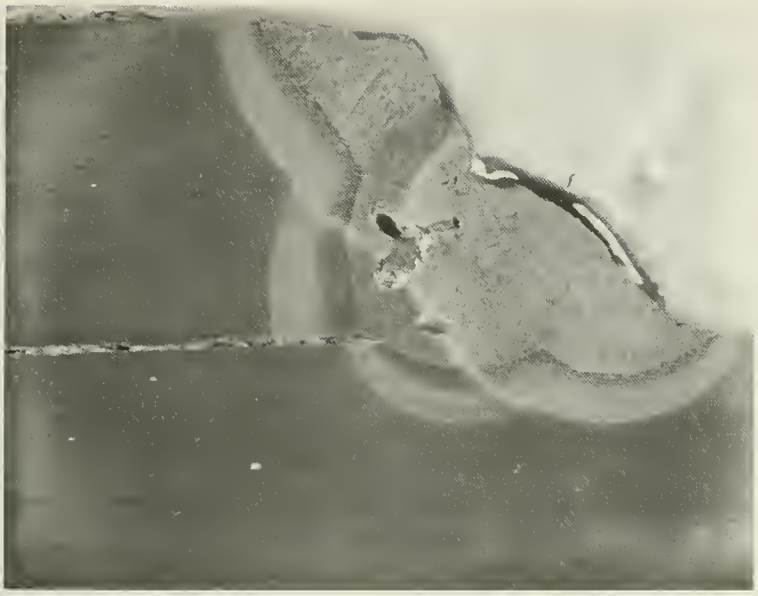

FIGURE 4-7: MULTI-PASS VERTICLE UNDERWATER WELDED LAP JOINT #3 USING E11018 ELECTRODE (5x, 2% NITAL)

FIGURE 4-8: LAP JOINT #3 SHOWING "FUSION" CRACKS IN THE WELD METAL NEAR THE HAZ (500x, 2% NITAL)

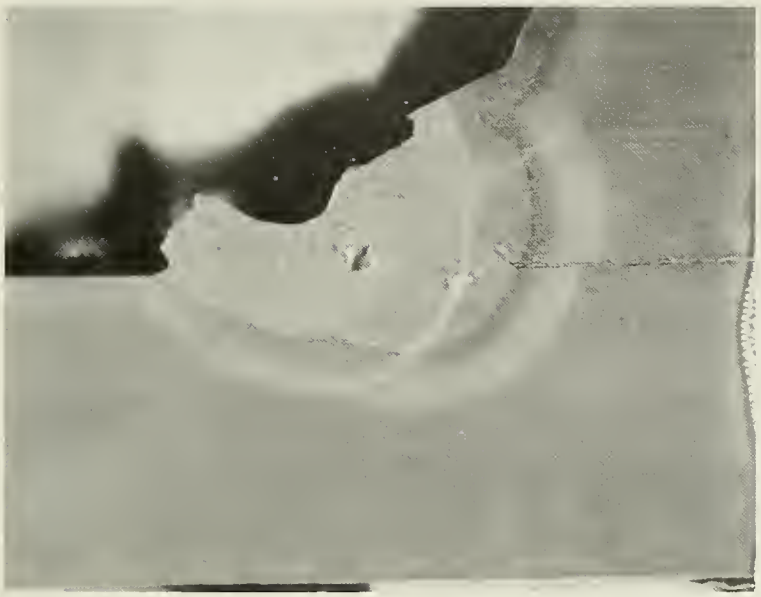

FIGURE 4-9: MULTI-PASS OVERHEAD UNDERWATER WELDED LAP JOINT #4 USING E11018 ELECTRODE (5x, 2% NITAL)

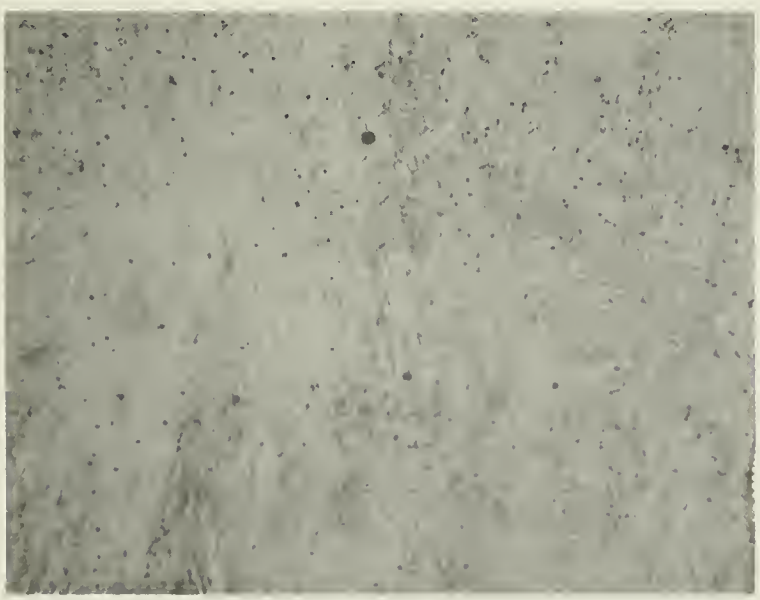

FIGURE 4-10: LAP JOINT #4 SHOWING EXTENSIVE POROSITY THROUGHOUT THE WELD METAL

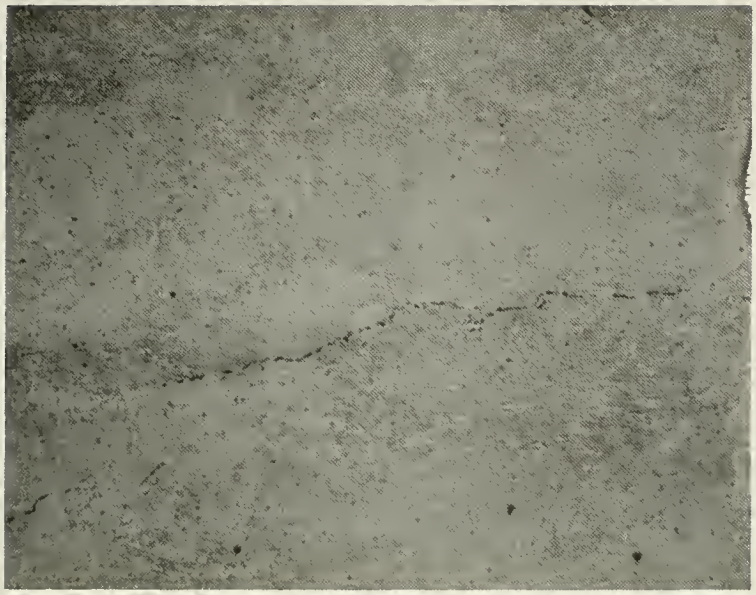

FIGURE 4-11: LAP JOINT #4 SHOWING EXTENSIVE POROSITY THROUGHOUT WELD METAL - NOTE THE JOINING OF THE PORES TO FORM A CRACK (100x, 2% NITAL)

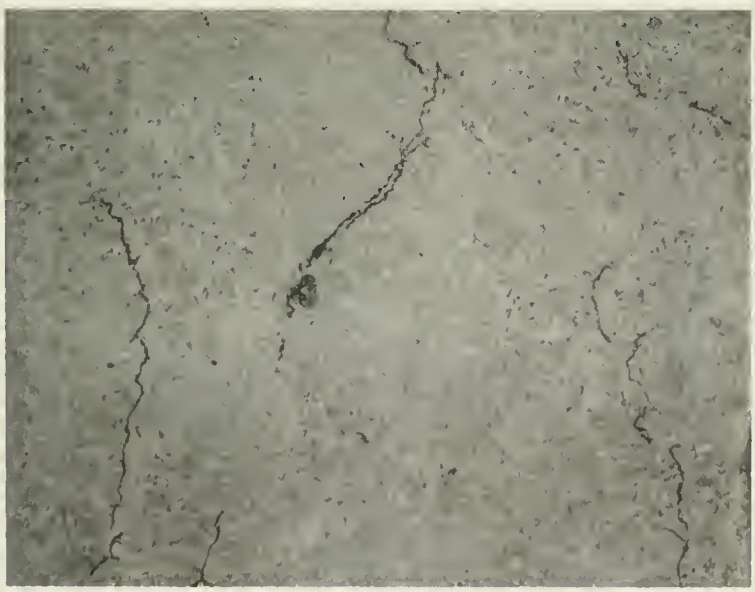

FIGURE 4-12: LAP JOINT #4 SHOWING "FUSION" CRACKS IN THE WELD METAL NEAR THE HAZ (100x, 2% NITAL)

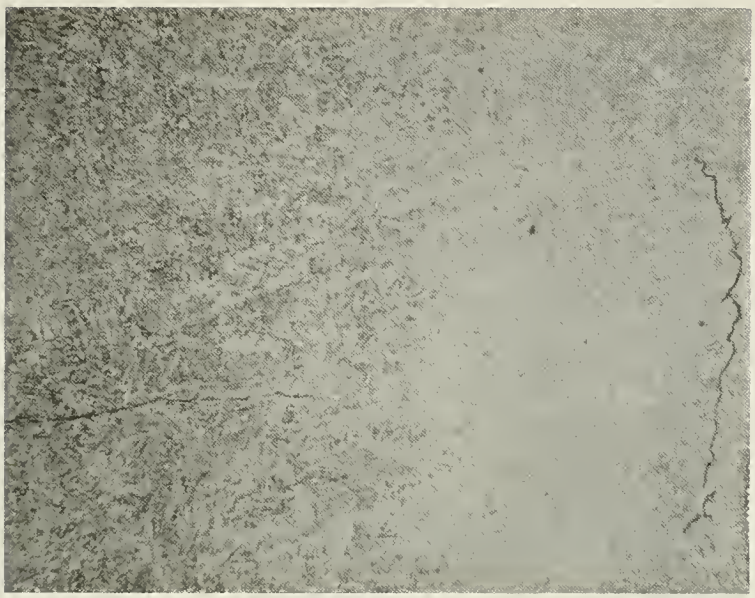

FIGURE 4-13: LAP JOINT #4 SHOWING A "FUSION" CRACK IN THE WELD METAL NEAR THE HAZ AND A "TRANSVERSE" CRACK INITIATING IN THE WELD METAL AND PROPAGATING INTO THE HAZ (100x, 2% NITAL)

FIGURE 4-14: MULTI-PASS OVERHEAD UNDERWATER WELDED LAP JOINT #5 USING E11018 ELECTRODE (5x, 2% NITAL)

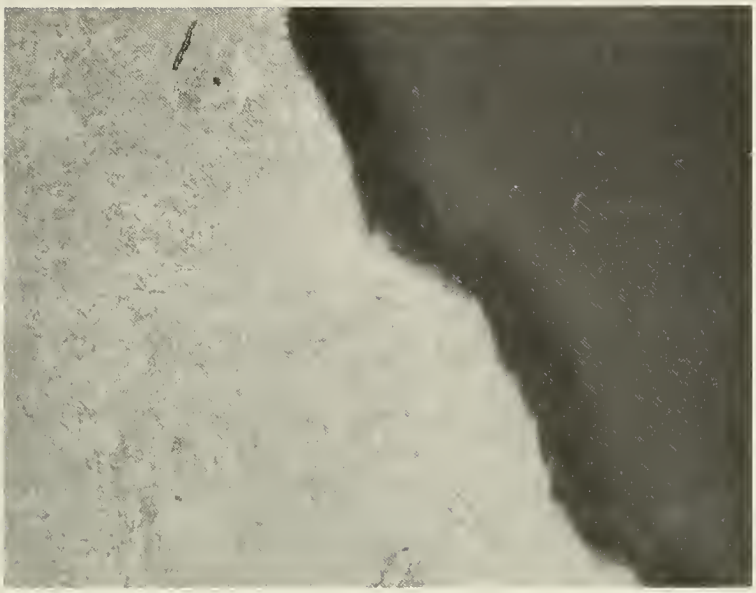

FIGURE 4-15: LAP JOINT #5 SHOWING NO CRACKING IN THE WELD METAL NEAR THE WATER ENVIRONMENT (100x, 2% NITAL)

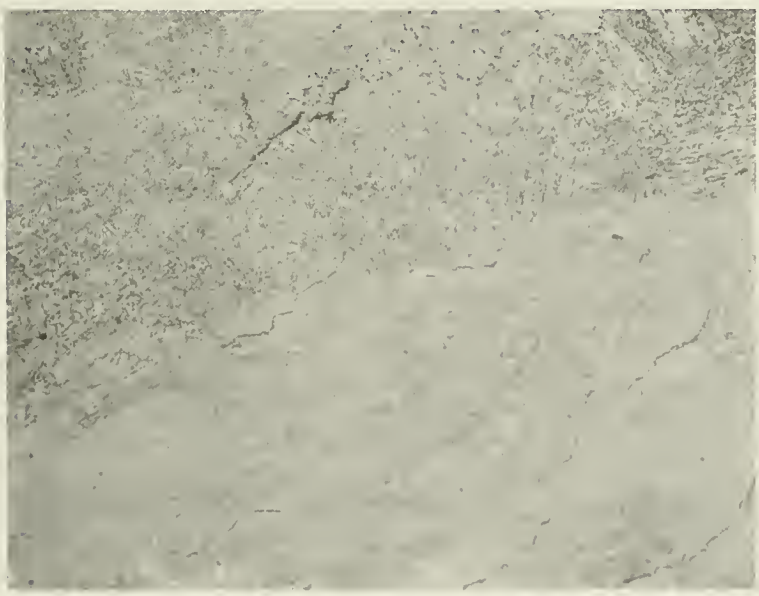

FIGURE 4-16: LAP JOINT #5 SHOWING "FUSION" CRACKS IN THE WELD METAL NEAR THE HAZ (100x, 2% NITAL)

CONCLUSIONS

The underwater welded HY-80 steel lap joints have not experienced the hydrogen embrittlement phenomena.

The cracks observed in the microscopic investigation were of the "fusion" and "transverse" type, as described by Cabelka[8]. These cracks occur in the weld metal, and in the case of the "transverse" cracks, can propagate into the heat affected zone, and possibly into the uneffected base metal. The "fusion" cracks are not dependent upon hydrogen for their initiation, but instead are the result of a combination of tensile stresses and a hard microstructure. "Transverse" cracks initiate in zones of "overheated martensite" and occur as a result of shrinkage stresses. They, also, are not dependent upon hydrogen for their formation.

The type of cracks which occur in welded HY-80 steel joints which experience the hydrogen embrittlement phenomena, underbead cracks, were not observed during the microscopic investigation.

Although the degree of porosity is extensive throughout the weld metal, it is a less critical weld defect and should be of less concern. Catastropic failure of the underwater welded HY-80 steel joint is more likely to occur as a result of the "fusion" cracks and the "transverse" cracks, than as a result of the porosity.

However, in order to determine the significance of the "fusion" cracks and the "transverse" cracks, it is necessary to know the properties of the residual stresses in the weld metal and the nature of the service required for the underwater welded HY-80 steel joint.

CHAPTER 5

MICROHARDNESS TEST

GENERAL

The microhardness tests of the underwater welded HY-80 steel lap joints were conducted on a Wilson Model LL Tukon Microhardness Tester located in the Material Science Department at M.I.T. A load of 500 grams was used for the tests. The resulting diamond imprint was microscopically measured in m, converted to a Knoop Hardness in Kg/mm, and then approximated to a Rockwell C value.

The microhardness test specimens were prepared from the underwater welded HY-80 steel doubler plate, shown in Figure 6-1.

TEST RESULTS

The results of the microhardness tests are shown in Figures 5-1 through 5-5. Each microhardness test specimen shown in the figures has been micro-polished with a 0.3 alumina/distilled water solution on a #600 polishing wheel and then etched with a 2% Nital solution.

HK = 478.0
R_c = 46

HK = 191.0
R_c = -

HK = 329.2
R_c = 32

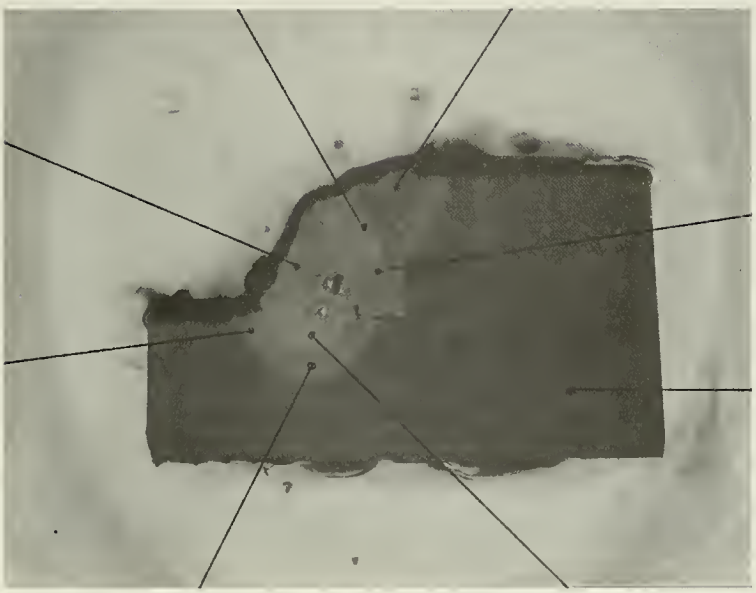

HK = 470.2
R_c = 47

HK = 470.2
R_c = 47

HK = 240.6
R_c = 17

HK = 441.0
R_c = 44.5

HK = 390.4
R_c = 39

FIGURE 5-1 : DOWNHAND WELDED MICROHARDNESS TEST SPECIMEN

HK = 528.5
R_c = 49

HK = 402.4
R_c = 40

HK = 373.6
R_c = 37

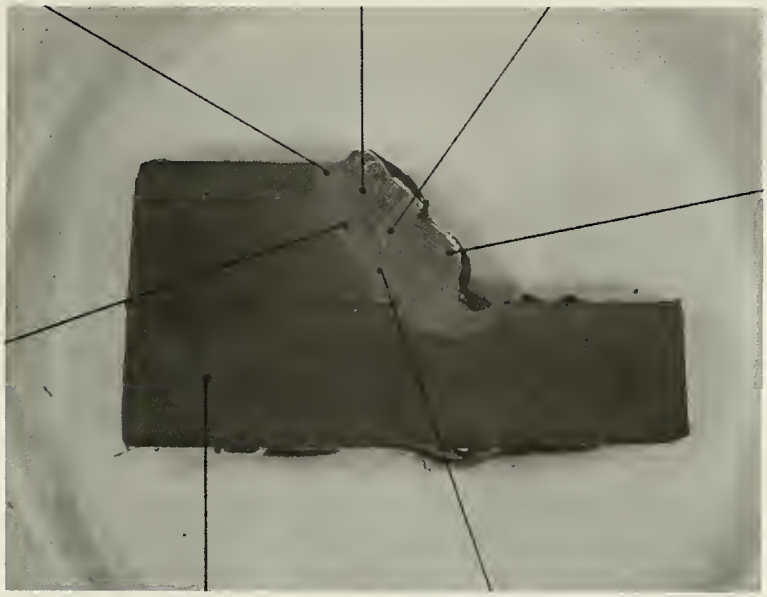

HK = 414.6
R_c = 41

HK = 478.0
R_c = 46

HK = 258.2
R_c = 21

HK = 538.0
R_c = 49.5

FIGURE 5-2: DOWNHAND WELDED MICROHARDNESS TEST SPECIMEN

HK = 441.0
R_c = 43

HK = 414.6
R_c = 41

HK = 421.0
R_c = 41.5

HK = 441.0
R_c = 43

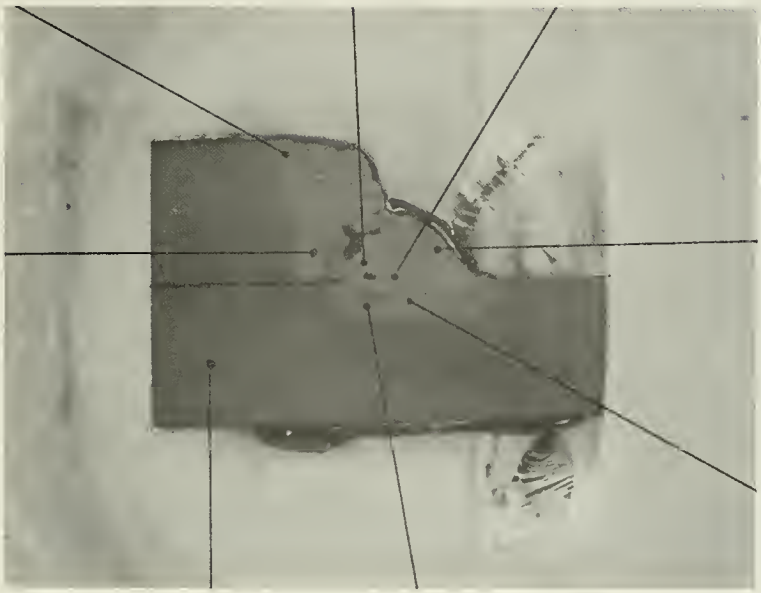

HK = 358.0
R_c = 36

HK = 486.0
R_c = 46.5

HK = 271.0
R_c = 24

HK = 455.2
R_c = 44

FIGURE 5-3: VERTICLE WELDED MICROHARDNESS TEST SPECIMEN

HK = 414.6
R_c = 41

HK = 421.0
R_c = 43

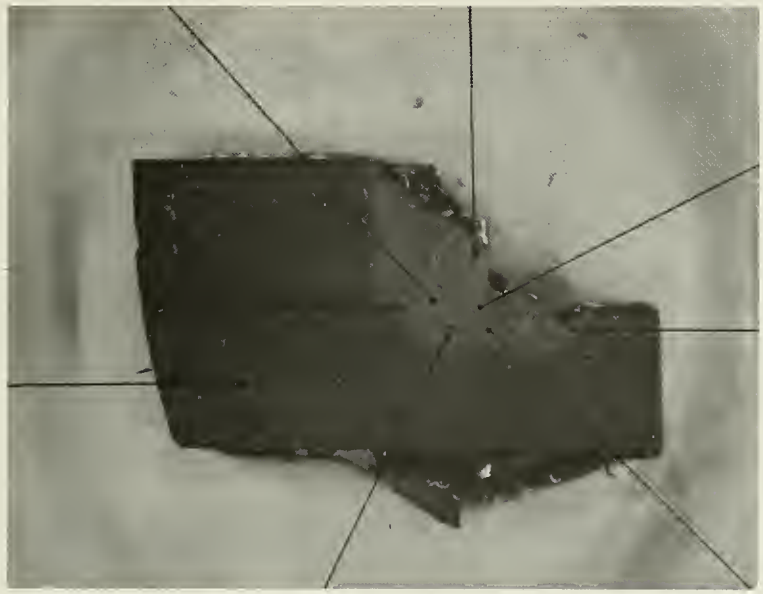

HK = 455.2
R_c = 44

HK = 448.0
R_c = 44

HK = 277.8
R_c = 25

HK = 373.6
R_c = 37

HK = 511.0
R_c = 48

FIGURE 5-4: OVERHEAD WELDED MICROHARDNESS TEST SPECIMEN

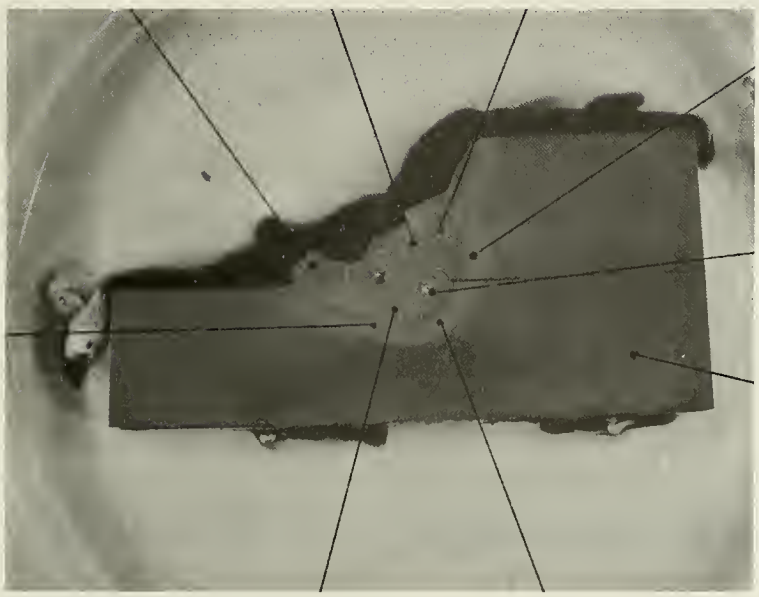

FIGURE 5-5: OVERHEAD WELDED MICROHARDNESS TEST SPECIMEN

CONCLUSIONS

The heat affected zone of subsequent passes in the multi-pass technique does not appear to temper the weld metal or heat affected zone of previous passes. In fact, the microhardness tests results seem to indicate that regions of heat affected zone and weld metal which fall within the heat affected zone of subsequent passes are actually hardened. This is not in agreement with Meloney[22], who concluded that the "multi-pass regions" experienced less hardness.

The hardness of the weld metal is greatest near the heat affected zone and decreases near the water. However, the hardness of the heat affected zone appears to increase nearer the water.

The regions of greatest microhardness should be the most susceptable to microcracking in the presence of tri-axial tensile stresses and hydrogen embrittlement.

CHAPTER 6

MECHANICAL BEND TEST

GENERAL

The mechanical bend tests of the underwater welded HY-80 steel lap joints were conducted on an Instrun test machine located in the Material Science Department at M.I.T. A guided bend test jig was used in conducting these tests.

The HY-80 steel lap joint bend specimens were prepared from the underwater welded HY-80 steel doubler plates as shown in Figure 6-1. The arrows on the doubler plates indicate the "north" direction of the plate during the underwater welding process.

TEST RESULTS

The results of the HY-80 steel lap joint bend tests are shown in Figures 6-2 through 6-12. The graphs shown were taken from the information charted by the Instrun test machine during the bend test of each HY-80 steel lap joint specimen. Each graph indicates the time to failure with a crosshead speed of 0.02 inches per minute, and the load necessary to cause the failure to occur.

In the case of the two overhead welded HY-80 steel lap joint specimens, the test results were quite different. Test specimen OH-1 experienced failure of the weld metal and complete fracture of

the specimen before any failure was initiated in the base metal. On the other hand, the weld area of specimen OH-2 was uneffected by the load.

In all the other cases of the HY-80 steel lap joint specimens, failure occurred at the toe of the weld and was of the Type '2' fracture, as described in MIL-STD-00418B (SHIPS). These results are in agreement with those observed by Meloney[22].

The surface of the Type '2' fractures and the OH-1 specimen appeared gray and silky with fibrous dimples indicating a ductile shear type fracture.

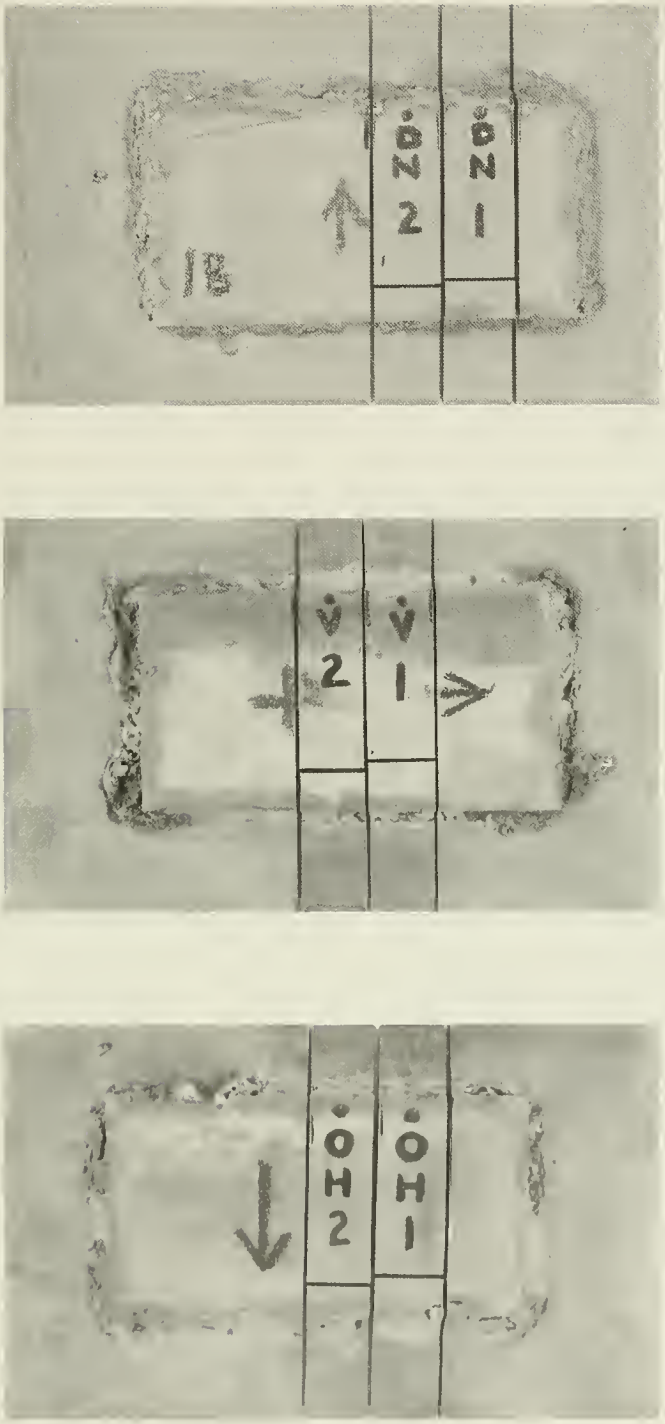

FIGURE 6-1: PREPARATION OF LAP JOINT BEND SPECIMENS

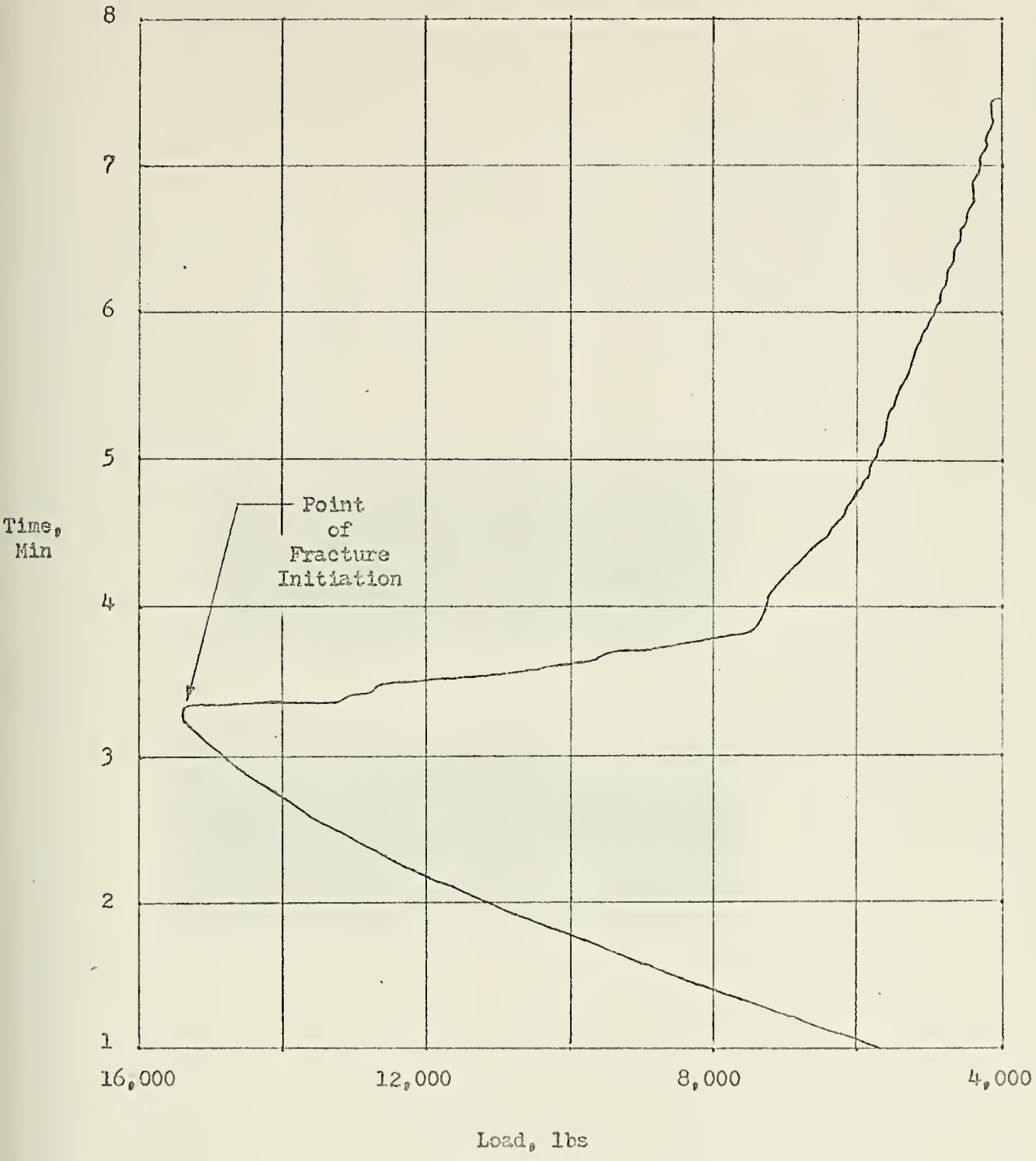

FIGURE 6-2: FAILURE CHARACTERISTICS OF DOWNHAND WELDED LAP JOINT BEND TEST SPECIMEN DN-J

FIGURE 6-3 : RESULTS OF BEND TEST ON DOWNHAND WELDED LAP JOINT
BEND TEST SPECIMEN DN-1

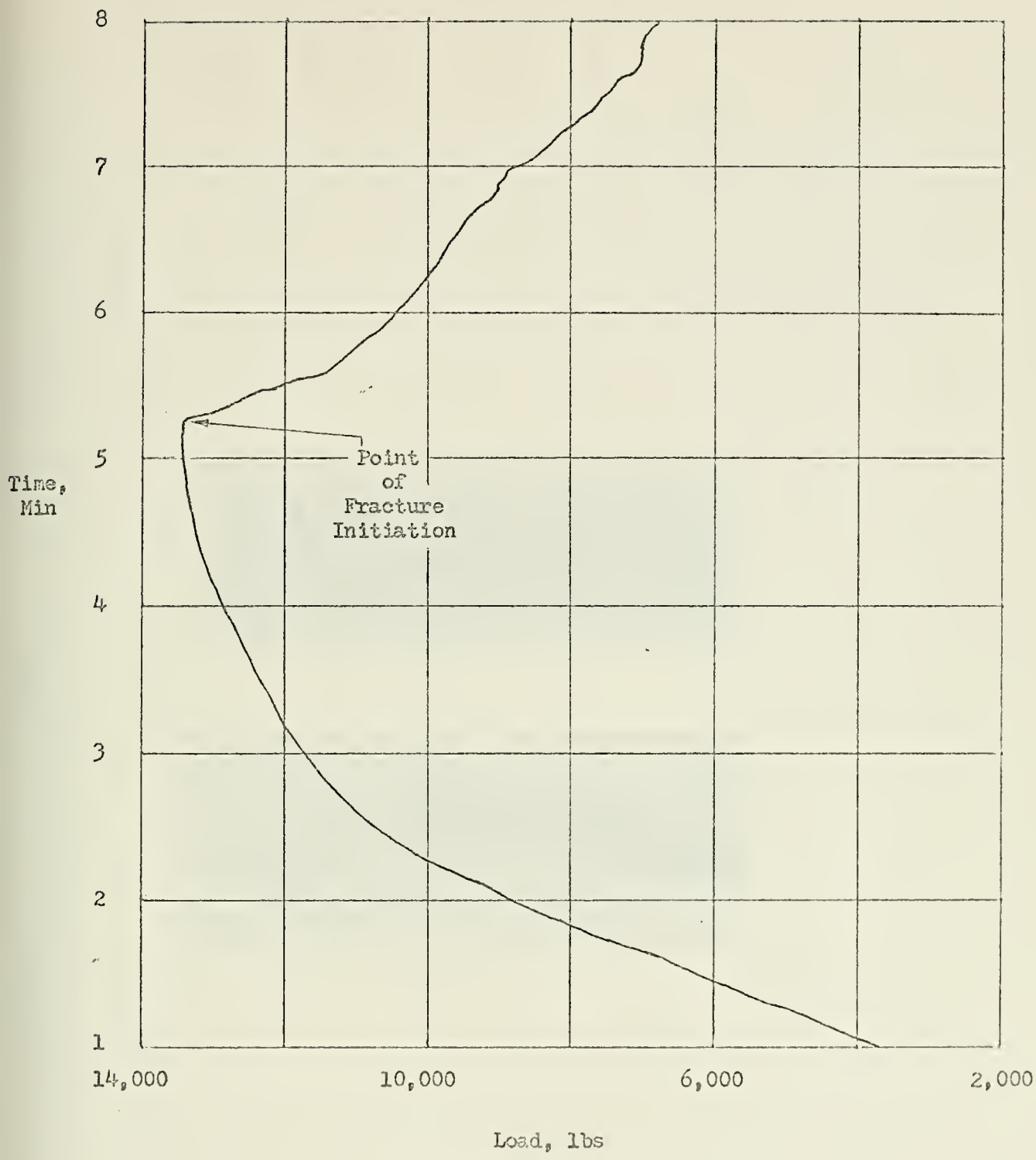

FIGURE 6-4 : FAILURE CHARACTERISTICS OF DOWNHAND WELDED LAP JOINT BEND TEST SPECIMEN DN-2

FIGURE 6-5 : RESULTS OF BEND TEST ON DOWNHAND WELDED LAP JOINT
BEND TEST SPECIMEN DN-2

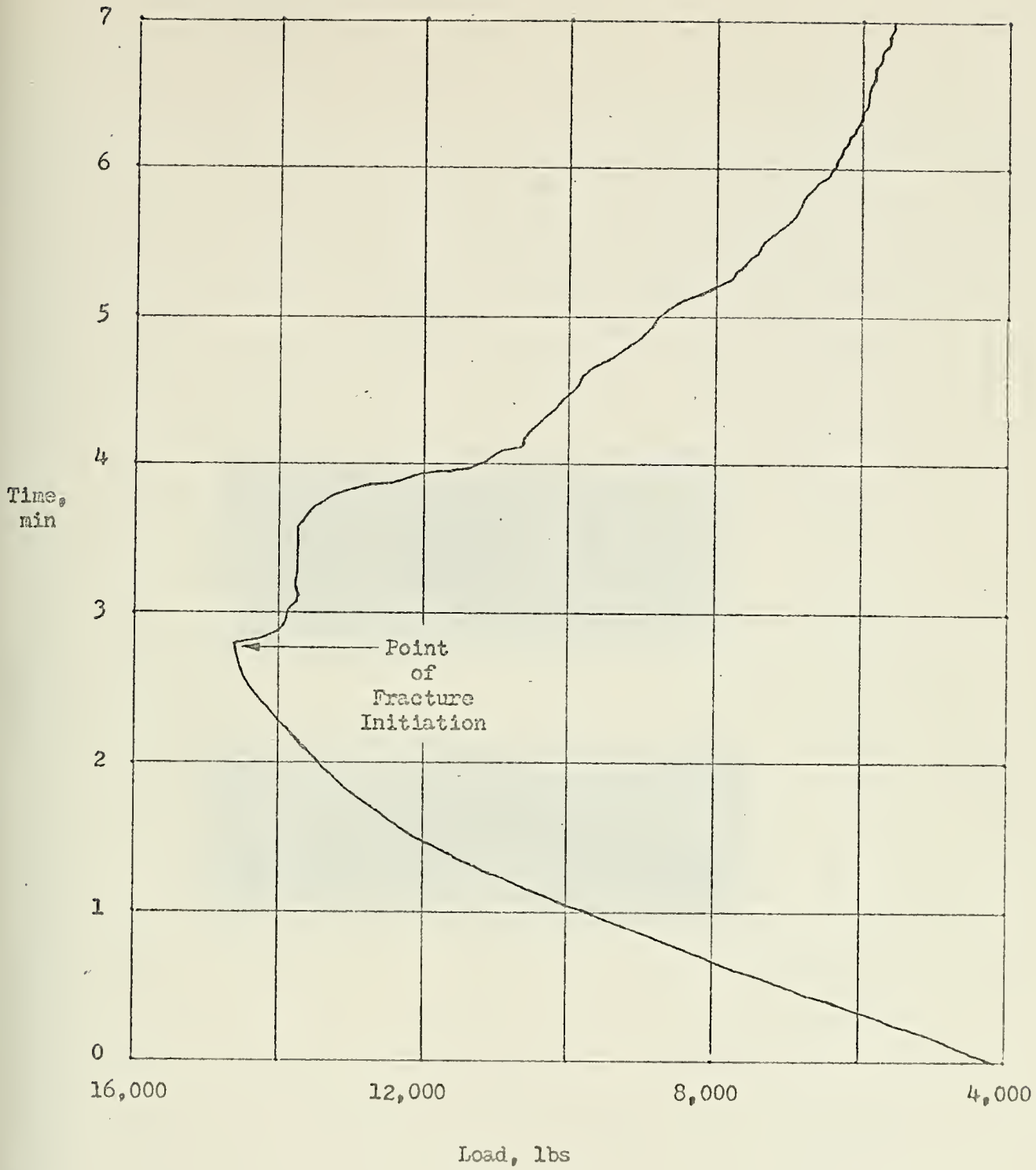

FIGURE 6-6 : FAILURE CHARACTERISTICS OF VERTICLE WELDED LAP JOINT BEND TEST SPECIMEN V-1

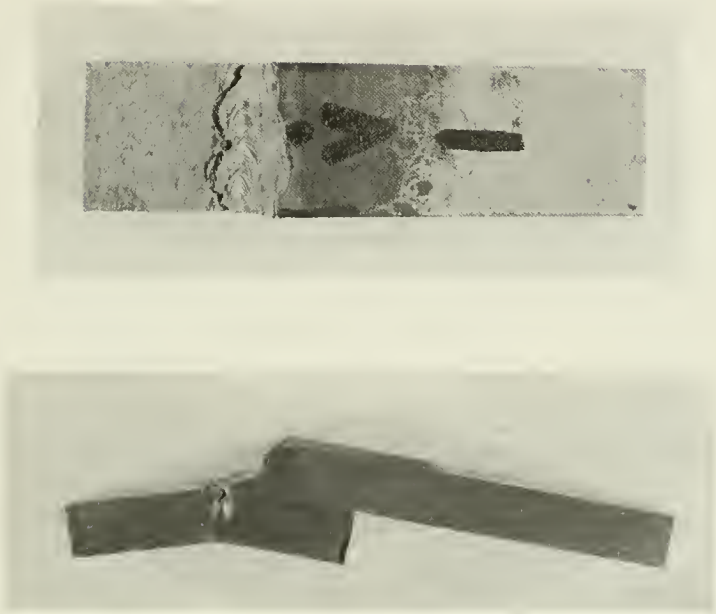

FIGURE 6-7 : RESULTS OF BEND TEST ON VERTICLE WELDED LAP JOINT
BEND TEST SPECIMEN V-1

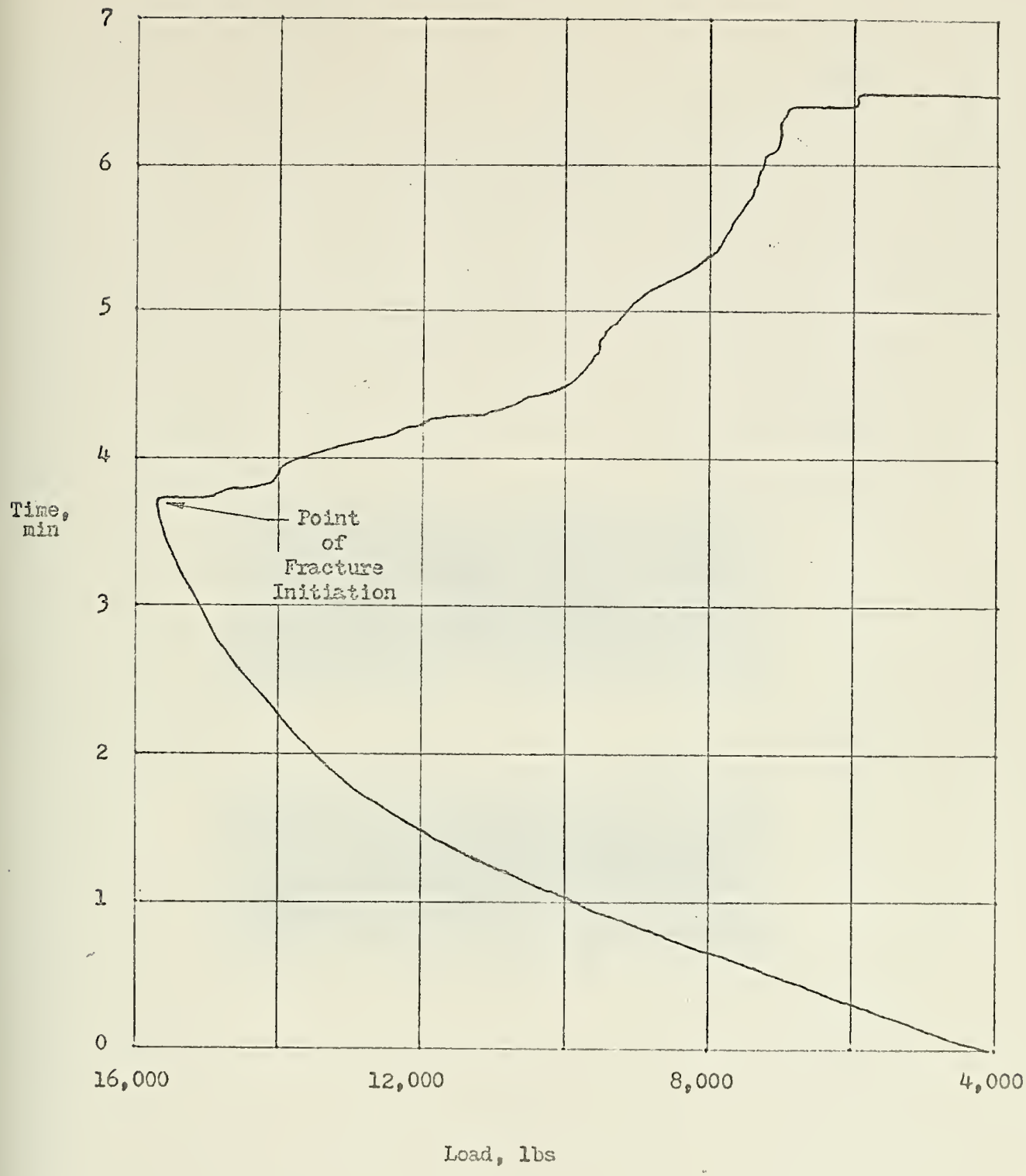

FIGURE 6-8 : FAILURE CHARACTERISTICS OF VERTICLE WELDED LAP JOINT BEND TEST SPECIMEN V-2

FIGURE 6-9 : RESULTS OF BEND TEST ON VERTICLE WELDED LAP JOINT
BEND TEST SPECIMEN V-2

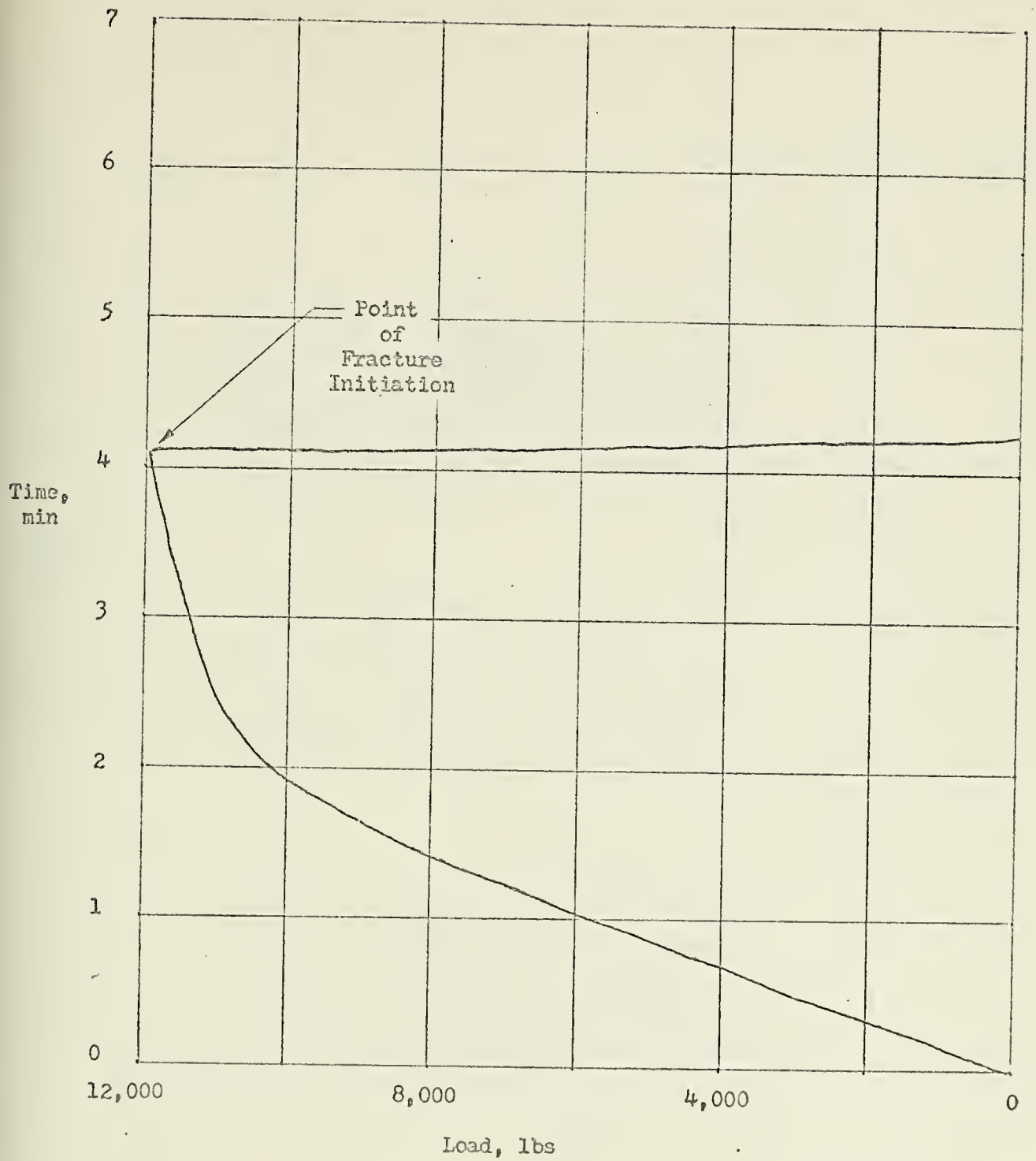

FIGURE 6-10: FAILURE CHARACTERISTICS OF OVERHEAD WELDED LAP JOINT BEND TEST SPECIMEN OH-1

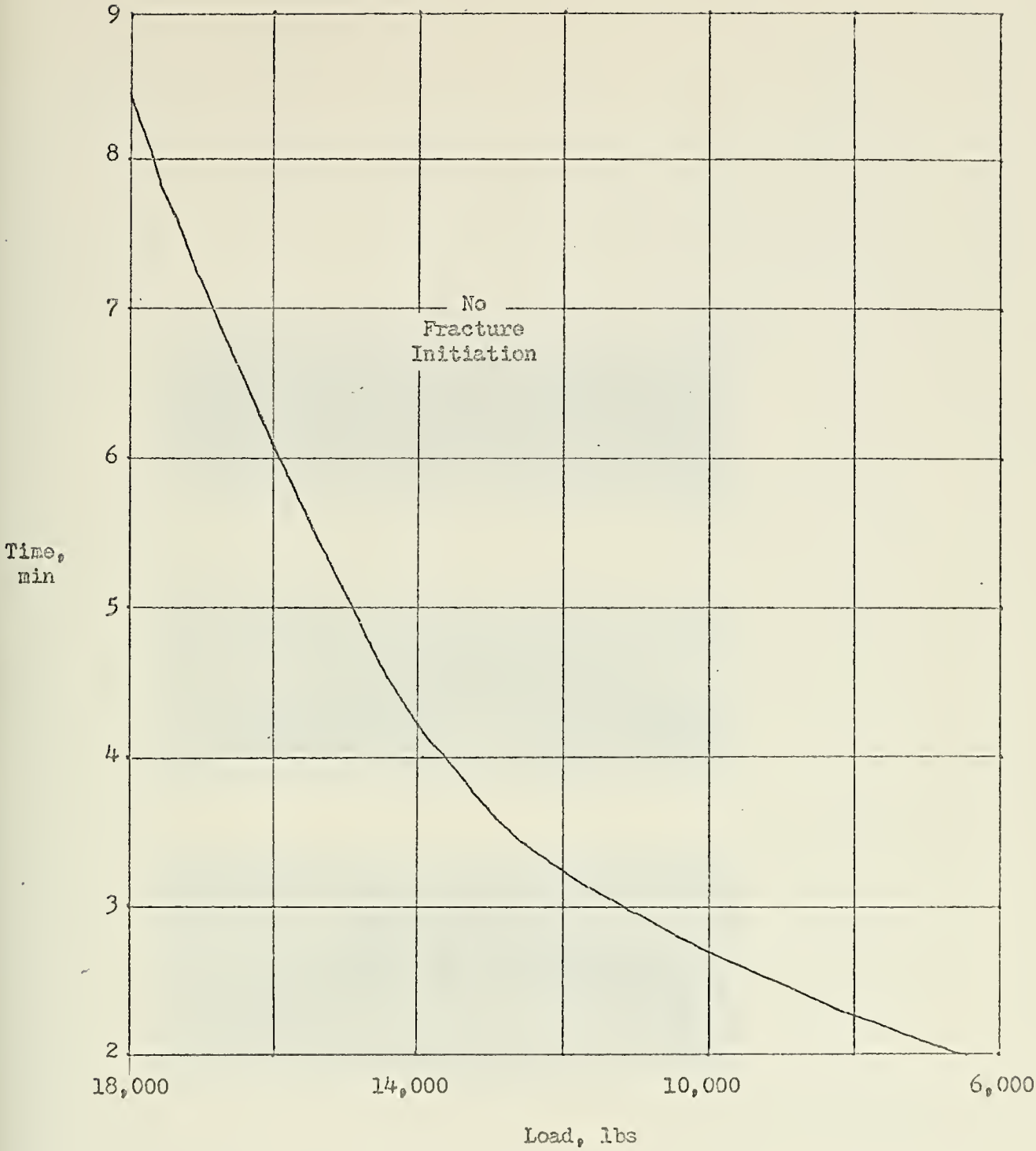

FIGURE 6-11: FAILURE CHARACTERISTICS OF OVERHEAD WELDED LAP JOINT BEND TEST SPECIMEN OH-2

FIGURE 6-12: RESULTS OF BEND TEST ON OVERHEAD WELDED LAP JOINT
BEND TEST SPECIMENS OH-1 and OH-2

CONCLUSIONS

Type '2' fractures, which initiate in the toe of the weld and propagate through the heat affected zone into the base metal, were experienced. These fractures were gray and silky in appearance with fibrous dimples, indicating a ductile shear type fracture.

Therefore, the weld metal near the heat affected zone, the heat affected zone, and the base metal near the heat affected zone, experienced ductile shear fracture, which continued to propagate slowly, even after the failure had been initiated and the load continued to be applied. There was no rapid propagation of the fracture or catastropic failure.

Thus it appears that the hydrogen embrittlement phenomena did not occur in the weld metal near the heat affected zone, the heat affected zone, or the base metal near the heat affected zone. The characteristics of a brittle cleavage fracture were not present, and rapid propagation of the crack, leading to a total failure, did not occur, even though the load continued to be applied after the fracture had been initiated.

The presence of hydrogen and the resultant hydrogen embrittle-

ment phenomena would have caused a loss in ductility and the retardation of plastic deformation. This occurance would result in a transition from a ductile shear fracture to a brittle cleavage fracture with rapid crack propagation and total failure with a continued applied stress.

This phenomena was not observed.

PART III

FINDINGS

CHAPTER 7

CONCLUSIONS

HYDROGEN EMBRITTLEMENT

Underwater welded HY-80 steel may not experience hydrogen embrittlement as may air welded HY-80 steel. This is true despite the fact that the weld metal of an underwater welded HY-80 steel joint contains pores of entrapped gas, whose major components are 70% H_2, 10% CO, and 20% other gases, and whose source is the bubble phenomena resulting from the dissociation of the water environment, which generates bubbles with a composition of 67-82% H_2, 11-24% CO, 4-6% CO_2, and 3% N_2, O_2, and metalic and mineral vapors.(4)

The bubbles generated by the dissociation of the water environment by the welding arc are entrapped by the rapidly solidifying molten weld metal. However, the hydrogen present in the pores does not appear to be absorbed and thus does not diffuse into the latice structure of the weld metal. The rapid temperature distribution, with time, during the underwater welding process, does not appear to provide sufficient energy for the molecular hydrogen entrapped in the pores of the weld metal, to be dissociated to atomic hydrogen and adsorbed by the atoms which form the surface layer of the pore. Without adsorption, absorption can not occur.

Assuming that some atomic hydrogen is present and adsorbed by the atoms which form the surface of the pore, absorption and diffusion

to the critical areas of tri-axial stresses are unlikely to occur. The rapid temperature distribution, with time, during the underwater welding process, and the below "room temperature" ambient temperatures, greatly reduce the diffusivity coefficient of the hydrogen. In addition, the rapid strain rate prevents what little hydrogen that may diffuse into the lattice structure from traveling to the critical areas of tri-axial stresses.

For the hydrogen embrittlement phenomena to occur, the progression of dissociation of molecular hydrogen to atomic hydrogen, adsorption by the atoms comprising the surface of the material, and absorption and diffusion of the hydrogen through the metal lattice structure to form hydrogen concentrations in the areas of tri-axial stress concentration, must be completed.

The experimental results indicate that this progression was not completed, and thus the conclusion that the underwater welded HY-80 steel lap joints have not experienced the hydrogen embrittlement phenomena.

The microscopic investigation revealed extensive porosity and "fusion" and "transverse" cracks in the weld metal, which occurred as a result of high tensile shrinkage stresses and hard microstructure. However, the microscopic investigation did not reveal any underbead

cracking in the heat affected zone, which also would have occurred as a result of the high shrinkage tensile stresses and hard microstructure, had hydrogen diffused into the region.

The ambiant temperature of the water environment during the underwater welding of the HY-80 steel doubler plates, and thus the water quench temperature of the welded joints, was 21.7°C (71°F). This temperature was sufficiently below "room temperature" to prevent the completion of the progression of hydrogen necessary for the hydrogen embrittlement phenomena to occur. Yet, the quench was severe enough to cause shrinkage tensile stresses high enough, that when combined with the hard microstructure, "fusion" and "transverse" cracks occurred.

These findings are supported by Kobayashi and Aoshima[18], who observed that for welded low alloy steels, quenched at a water temperature below 25°C (77°F), hydrogen diffusion is retarded and the progression of hydrogen necessary for the hydrogen embrittlement phenomena to occur, is prevented from going to completion. However, non-hydrogen induced cracks occurred as a result of the high thermal stresses caused by the rapid quench. Kobayashi and Aoshima[18] also observed that at water quench temperatures above 50°C (122°F), hydrogen diffusion is advanced to a degree that it is able to overcome the affinity of hydrogen for areas of high stress concentration. Thus

the progression of hydrogen necessary for the hydrogen embrittlement phenomena to occur is once again prevented from going to completion.

This upper limit for the hydrogen embrittlement phenomena observed by Kobayashi and Aoshima[18] is supported by the minimum preheat and interpass temperatures requirement for the welding of HY-80 steel, which is set at 51.7°C (125°F).

Thus, HY-80 steel may be welded underwater without concern for the hydrogen embrittlement phenomena, providing the temperature of the water environment, and thus the water quench temperature, is below 25°C (77°F). And from the work of Kobayashi and Aoshima[18] and Cabelka[8], it appears that this conclusion can be applied to other low alloy steels.

At a water environment temperature of 25°C (77°F) and below, the concern in the underwater welding of HY-80 steel, and other low alloy steels, is the same as that for welding mild steel, the rapid quenching and the resultant combination of hard microstructure and high shrinkage tensile stresses. However, before any definitive statements can be made in this area, it will be necessary for a study of the thermal stresses encountered during the underwater welding process to be conducted.

Suggestions have been made by Brown, et al[4], and Meloney[22] that strip heaters, or some other form of preheat and interpass heat, be developed for the underwater welding process, in an effort to reduce the effects of the rapid temperature distribution, with time. In an effort to reduce these effects, which do not appear to be critical to the accomplishment of an effective underwater weld, as is supported by Grubbs and Teth[15], the conditions could be created to allow for the hydrogen embrittlement phenomena to occur. Thus a critical situation which does not exist, may be created in an attempt to reduce the effects of a non-critical condition.

UNDERWATER WELDING EXPERIMENT

The greatest difficulty encountered in performing the underwater welding of the HY-80 steel doubler plates was that of freedom of motion. The restrictions of the Navy Standard MKV hard hat diving system was the major factor effecting the outcome of the underwater welding operation. The planned adoption of the MKX hard hat diving system as a replacement for the Navy Standard MKV hard hat diving system should overcome this difficulty, since it will provide the diver with a greater degree of mobility and dreedom of motion.

The problem of visibility that has been encountered by Brown[4] and Meloney[22] was not encountered. By tho welder being a diver

and in the water with the HY-80 steel joint to be welded, the welder was not forced to look down through the bubbles and turbidity generated by the welding arc. By being in the water, the welder was able to position himself so that the joint to be welded was at eye level, and thereby eliminate the effect of the bubbles and turbidity.

This situation enabled the welder to have a clear view of the joint to be welded and to manipulate the welding electrode, within the limits imposed by the Navy Standard MKV hard hat diving system. It was, therefore, possible to perform the multi-pass technique in the downhand, verticle, and overhead welding positions, and to attempt the temper bead technique. These techniques were also possible within the limits imposed by the Navy Standard MKV hard hat system.

The quality of the underwater welded HY-80 steel lap joint was effected by the inability to completely remove the slag after each pass, before laying the subsequent pass, in the multi-pass technique. Sufficient striking force could not be applied with the hand tools available, therefore a scraping technique was used. This did not result in the complete removal of the slag and thus the greatly reduced weld quality. This condition could be overcome by the use of pneumatic or hydraulic hand tools for the chipping of the slag from the weld metal and the grinding of the weld metal surface before laying the subsequent pass in the multi-pass technique. This factor

was identified by Rothman and Monroe[25] as playing a major role in the performance of an acceptable underwater weld. With the distribution of the new diver's hydraulic tool package, developed by the Naval Coastal Systems Laboratory, this problem should be solved.

SUMMARY

With the adoption of the MKX hard hat system, the availability of the diver's hydraulic tool package, a naturally clear water environment, and the proper training, the diver-welded should be able to perform an acceptable underwater weld of HY-80 steel, free from the hydrogen embrittlement phenomena and within the joint efficiencies described by Meloney[22]. From the findings of Kobayashi and Aoshima[18] and Cabelka[8], this capability should also be able to be applied to other low alloy steels.

The question that still has to be answered is the consequences of the combination of the high shrinkage tensile stresses and the hard microstructure. For this to be answered the properties of the residual stresses must be determined and their effect considered in light of the service life required of the joint.

CHAPTER 8

RECOMMENDATIONS

GENERAL

Maloney[22] has shown that underwater welded HY-80 steel joints can be fabricated, under laboratory conditions, with properties that are acceptable for repair welds. This work has been extended by the author, who has shown that underwater welded HY-80 steel joints can be fabricated, under working conditions, without hydrogen embrittlement, using presently available equipment, within the present guidelines established by the United States Navy for underwater welding operations.

Now that this capability has been established, work should be undertaken to optimize the underwater welding process for HY-80 steel and other low alloy steels.

PROCEDURE

When the MKX hard hat diving system is adopted by the United States Navy, and the diver's hydraulic tool package is available, additional working dives, for the purpose of underwater welding various HY-80 steel and other low alloy steel joints, should be performed. Included in the joints to be welded should be butt joints, as well as tee joints and lap joints. All of these joints should be welded in all positions using the multi-pass technique. These

working dives should explore various joint configurations for each type of joint and various weld pass preparation techniques. This may enable the underwater welding of HY-80 steel and other low alloy steel joints to be expanded from the relm of repair into that of fabrication.

The increased freedom of motion allowed by the MKX hard hat diving system and the capabilities provided by the diver's hydraulic tool package, should enable the properly trained diver-welded to perform these working dives.

ANALYSIS

Preheat and Interpass Heat. The effects of preheat and interpass heat on the rapid temperature distribution, with time, and thus the thermal stresses, in the region of the weld zone should be investigated. However, this investigation should be conducted in the light of the possible effect of preheat and interpass heat on the hydrogen embrittlement phenomena. The study should be conducted to determine if it is also possible to elevate the temperature of the weld zone above the region of critical hydrogen embrittlement, while attempting to overcome the effects of the rapid temperature distribution, with time, or whether a possibly non-critical condition will be corrected only to create a critical one.

Thermal Stresses. An investigation of the thermal stresses occuring during the underwater welding process should be conducted, in order to determine their contribution to the mechanical characteristics of the cracking of the underwater welded joint. By utilizing the information techniques developed by Ueda and Yamakawa[28], Fujita and Nomoto[14], and Brown[4], a thermal elastic-plastic analysis of the underwater welded joint could be conducted. As a result of this investigation, it should be possible to make a definitive statement as to the effect of the temperature change, with time, and the resultant thermal stresses, on an underwater welded joint, with regard to specific joint service life requirements.

PART IV

APPENDIXES

APPENDIX A

METALLURGY OF HY-80 STEEL

COMPOSITION

HY-80 is a low-carbon Ni-Cr-Mo steel which has a good combination of strength and toughness obtained through quench-and-tempering heat treatment. It is available under the military specifications:

1. Plate - MIL-S-16216
2. Extrusions - MIL-S-22664
3. Rolled Sections - MIL-S-22958
4. Castings - MIL-S-23008
5. Forgings - MIL-S-23009

and the commercial grades are covered by the ASTM specifications:

1. Plate - A543
2. Forgings - A541 and A508

The chemical composition of HY-80 steel as is specified by MIL-S-16216 and A543 and a typical HY-80 steel chemical composition are shown in Table A-1.

The amount of total sulphur and phosphorus content is limited in order to minimize the detrimental effects of these elements during welding. Additional control of the effect of sulphur is the primary reason for the use of Manganise. Molybdenum is used to increase the hardinability and increase the temper resistance by retarding the softening of the steel during tempering at high temperatures. Nickel contributes to the excellent toughness of

Element	Specifications		Typical
	MIL-S-16216	A543 (Grade A)	
Carbon[a]	0.18 max	0.23 max	0.16
Manganese	0.10 - 0.40	0.40 max	0.28
Silicon	0.15 - 0.35	0.20 - 0.35	0.23
Nickel	2.00 - 3.25	2.60 - 3.25	2.97
Chromium	1.00 - 1.80	1.50 - 2.00	1.68
Molybdenum	0.20 - 0.60	0.45 - 0.60	0.45
Phosphorus[b]	0.025 max	0.035 max	0.015
Sulphur[b]	0.025 max	0.040 max	0.16
Titanium	0.02 max	---	0.005
Vanadium	0.03 max	0.03 max	0.005
Copper	0.25 max	---	0.05
Iron	Remainder	Remainder	

(a) 0.20 max for plates 6 inches thick or greater

(b) The percent of combined phosphorus and sulpher shall be 0.045 max

TABLE A-1: CHEMICAL COMPOSITION OF HY-80 STEEL PLATE[13]

HY-80 steel and has a secondary effect of increasing the hardenability. Silicon is used primarily as a deoxidizer.

The wide range of variance for several of the elements shown in Table A-1 is to permit the steel manufacturer to adjust the hardenability of the steel to the thickness of the plate being produced. The greater the thickness of the plate being produced the greater the amount of alloying elements needed to obtain the desired hardenability.

METALLURGICAL CHARACTERISTICS

The microstructure of HY-80 steel is a combination of tempered bainite and tempered martensite in all section thicknesses.

MIL-S-16216 imposes two limitations on the steel manufacturer:

1. The final tempering temperature shall not be less than 1100°F.
2. The microstructure at the mid-thickness of the plate must contain not less than 80% tempered martensite.

The actual procedure to be followed during the final quench-and-tempering heat treatment is left to the discretion of the steel manufacturer as long as these two limitations are satisfied.

The procedure that is usually followed in the heat treatment

of HY-80 generally consists of austenitization at approximately 1650°F, followed by a water quench, followed by tempering at approximately 1150°F, followed by a second water quench.

Figure A-1 gives a representative time-temperature-transformation curve for different chemical compositions of HY-80 steel with different austenitization temperatures. It can be seen in this figure that there is an increase in the transformation time and the M_s temperature resulting from an increase in the austenitization temperature.

MECHANICAL PROPERTIES

The mechanical properties of HY-80 steel as is required by MIL-S-16216 and A543 and typical properties of a HY-80 specimen are shown in Table A-2. The Charpy V-Notch impact requirements are shown in Table A-3 and Figure A-2 shows the typical relationship of Charpy V-Notch energy versus temperature for a one (1) inch HY-80 steel plate sample.

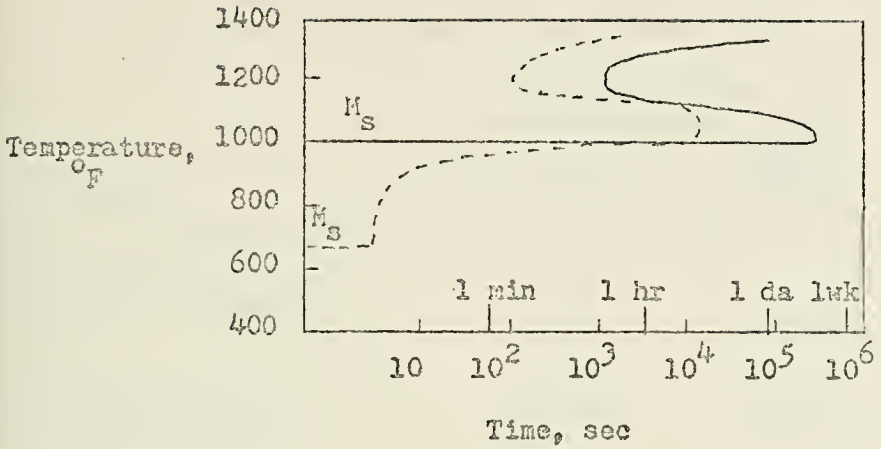

	Solid Curve	Dotted Curve
C	0.16	0.13
Mn	0.34	0.16
P	0.014	0.009
S	0.024	0.013
Si	0.25	0.10
Ni	2.87	3.08
Cr	1.52	1.76
Mo	0.41	0.49
Austenitizing Temperature	2400°F	1650°F

FIGURE A-1: TIME-TEMPERATURE-TRANSFORMATION DIAGRAMS FOR HY-80 STEEL SHOWING THE BEGINNING OF TRANSFORMATION (13)

Property	Specifications		Typical Value
	MIL-S-16216	A543 (Grade A)	
Tensile strength, ksi	NS[a]	105/125	111.5
Yeild strength 0.2% Offset, ksi	80/95[b]	85 min	95.5
Elongation in 2 in., min percent	20[b]	14	25.0
Reduction in area, percent			
Longitudinal	55[b]	NS	
Transverse	50[b]	NS	

(a) NS - not specified

(b) - These values for plate thickness 5/8 inch and greater

TABLE A-2: SPECIFICATION LIMITS FOR MECHANICAL PROPERTIES OF HY-80 STEEL (13)

Plate Thickness	Impact Strength, ft-lb, min
1/4 to 1/2 in. Excl.	(a)
1/2 to 2 in. Incl.	50 at -120°F
Over 2 in.	30 at -120°F

(a) Tests with the half-size Charpy specimen (10x5mm) are required for information only. Tests are not required for materials less than 1/4 inch thick.

TABLE A-3: CHARPY V-NOTCH IMPACT REQUIREMENTS FOR HY-80 STEEL PLATE UNDER SPECIFICATION MIL-S-16216 (13)

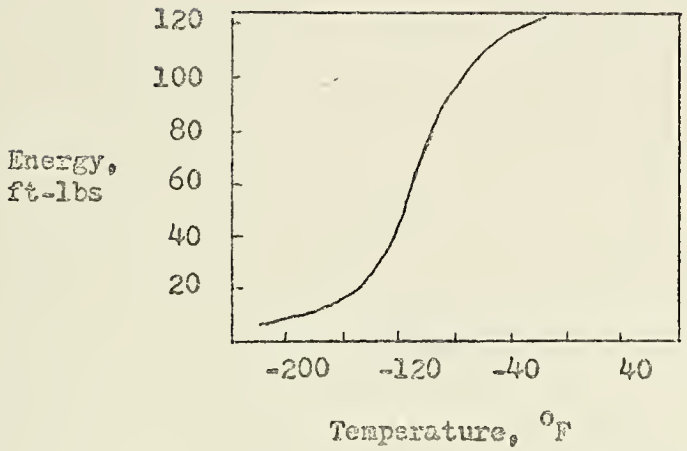

FIGURE A-2: TYPICAL RELATIONSHIP OF CHARPY V-NOTCH ENERGY TO TEST TEMPERATURE FOR 1-INCH THICK HY-80 STEEL PLATE (13)

APPENDIX B

WELDING OF HY-80 STEEL

SHIELDED METAL-ARC WELDING

The shielded metal-arc (SMA) fusion welding process uses an electrode which consists of a solid core wire covered with an extruded layer of flux. This flux is an important factor in the fusion welding process in that its composition is a controlling factor in such things as:

1. Arc stability
2. Weld metal composition
3. Fluxing and protection of molten metal
4. Weld-metal composition
5. Type of current
6. Properties of the slag produced
7. Bead contour
8. Welding position

Each of these elements of SMA fusion welding are shown in Figure B-1.

ELECTRODES

The SMA fusion welding of HY-80 steel requires a"low-hydrogen" type electrode. These electrodes are available under commercial specifications such as American Welding Society (AWS) and government specifications such as MIL-E-22200, and are recognized by the digits 15, 16, and 18 in the designations. Table B-1 gives the flux composition ranges for these "low-hydrogen" type electrodes in accordance with American Welding Society specifications.

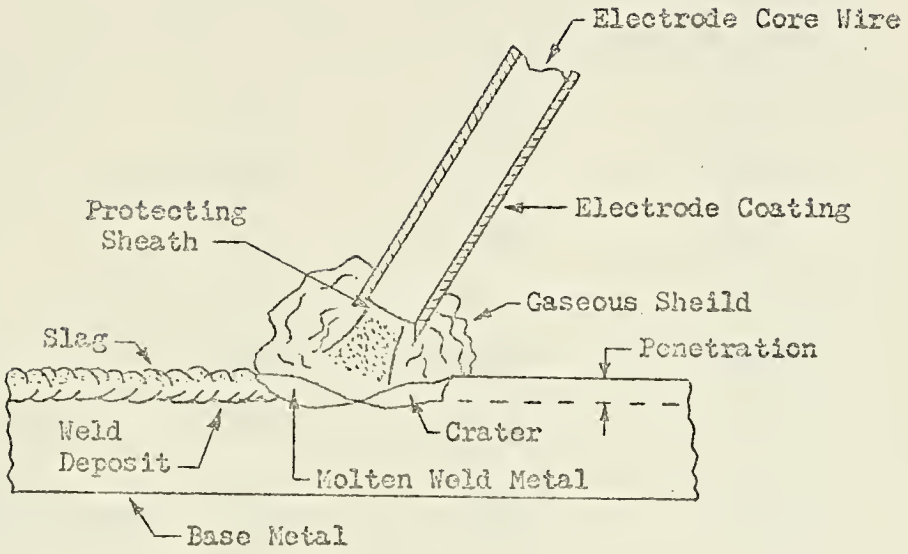

FIGURE B-1: ELEMENTS OF COVERED ELECTRODE SMA FUSION WELDING[13]

	AWS Class and Type of Coating, Weight (%)		
	Lime (E-XXX15)	Titania (E-XXX16)	Iron-Powder (E-XXX18)
Calcium Carbonate	10-30	10-30	10-30
Fluorspar	10-30	10-30	10-30
Titanium Oxide	0-8	15-30	0-8
Iron Powder	0-5	0-5	15-30
Ferro Alloys	15-30	15-30	15-30
Mineral Silicates	5-10	5-10	5-10
Sodium and/or Potassium Silicate	5-15	5-15	5-15

TABLE B-1: COMPOSITION RANGES OF COATINGS FOR LOW-HYDROGEN COVERED ELECTRODES (13)

The E-XXX15 electrodes are used with direct-current reverse polarity (DCRP) and utilize sodium silicate as the binder in the flux. The E-XXX16 electrodes utilize potassium silicate as the binder in the flux. This modification in the make up of the flux enables the E-XXX16 electrodes to be used with alternating-current as well as direct-current reverse polarity. Iron powder is added to the E-XXX18 electrodes which results in an improvement in the deposition efficiency and gives a quieter arc with less spatter. E-XXX18 electrodes are used with either alternating-current or direct-current straight polarity (DCSP).

The impact properties of the weld metal deposited with each of the "low-hydrogen" type covered electrodes are shown in Figure B-2. The iron-powder electrodes welds exhibit a greater toughness than the other "low-hydrogen" type covered electrodes and are thus generally used for the SMA fusion welding of HY-80 steel.

Typical impact properties of SMA fusion weld metal deposits in HY-80 steel using E-XXX18 iron-powder electrodes are shown in Table B-2. Typical mechanical of these weld deposits are shown in Table B-3.

The variation in the properties of the SMA fusion weld metal deposits shown in Figure B-2, Table B-2, and Table B-3 are generally due to the variations in the chemical composition of the covered electrode flux.

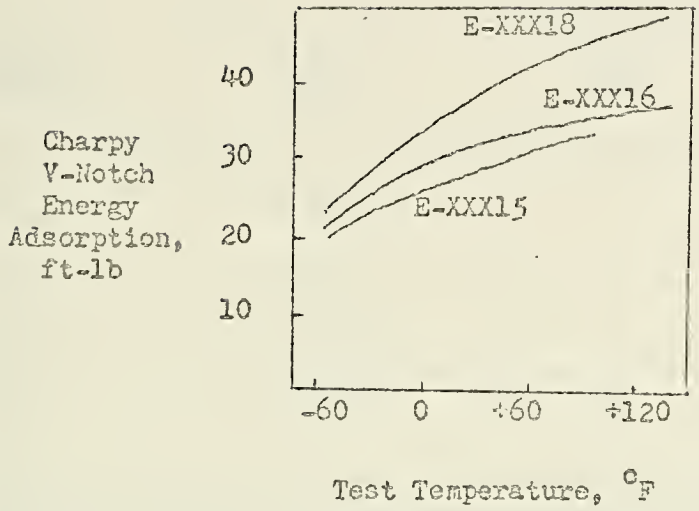

FIGURE B-2: IMPACT PROPERTIES OF WELD METALS DEPOSITED WITH EACH OF THE THREE "LOW-HYDROGEN" COVERED ELECTRODES (13)

Specimen Type(a)	Electrode Type	Impact Strength, ft-lb		
		30°F	0°F	-60°F
W	E-9018	--	--	62
W	E-9018	--	--	82
W	E-11018	--	--	45
T	E-11018	56	46	--

(a) Joint Type - T transverse butt-welded plate

W all weld-metal specimen

TABLE B-2: CHARPY V-NOTCH IMPACT PROPERTIES OF SMA WELDS DEPOSITED IN HY-80 STEEL WITH E-9018 and E-11018 ELECTRODES (13)

Specimen Type(a)	Electrode Type	Yeild Strength 0.2% Offset, ksi	Tensile Strength, ksi	Elongation in 2 inches, %
W	E-9018	81.5	91.1	26
W	E-9018	91.7	100.8	19.7
W	E-11018	108.5	113.0	22
W	E-11018	105.0	117.0	25
T	E-11018	89(b)	112.0	21

(a) Joint Type - T transverse butt-welded plate

W all weld-metal specimen

(b) Fractured in base metal

TABLE B-3: MECHANICAL PROPERTIES OF SMA WELDS DEPOSITED IN HY-80 STEEL WITH E-9018 AND E-11018 ELECTRODES (13)

WELDING REQUIREMENTS

The SMA fusion welding of HY-80 steel requires strict adherance to the requirements for a minimum preheat and interpass temperature and a maximum preheat and interpass temperature, as outlined in Table B-4.

The required preheat and interpass temperature may be obtained by the application of any of the following techniques, either singularly or in combination:

1. Resistance heaters
2. Radiant and/or infro-red heaters
3. Electrical induction
4. Soft-gas torch (gas-air)
5. Oxy-fuel torch

Application of the heat necessary to maintain the required preheat temperature must also be accomplished in a specified manner. A prime requirement is that the heat applied to be of the uniform, soaking type, thereby assuring that the entire welding area is brought up to the required minimum temperature while at the same time assuring that the specified maximum temperature is not exceeded at any local area. Once the minimum preheat temperature is established prior to the commencement of welding, it should be continuously maintained until the completion of the welding. Cyclic heating and the occurrence

Thickness	Minimum Preheat and Interpass Temperature	Maximum Preheat and Interpass Temperature
1-1/8 inch and over	200°F	300°F
over 1/2 inch but less than 1-1/8 inch	125°F	300°F
1/2 inch or less	60°F	300°F

TABLE B-4: MINIMUM AND MAXIMUM PREHEAT AND INTERPASS TEMPERATURE FOR WELDING HY-80 STEEL (12)

of temperature differentials of more than 100°F along the area to be welded are to be avoided.

Should the actual preheat temperature drop 75°F or more below the minimum specified, all partially completed welds are to be subjected to a magnetic particle inspection or liquid dye penetrant inspection where applicable. If the completed welds are found to be sound, the entire welding area is to be returned to the minimum preheat temperature prior to the resumption of welding.

The necessary control of the interpass temperature is to be accomplished by the proper distribution of welders and/or by the use of proper welding sequence.

Preheat and interpass temperatures are to be checked prior to the commencement of welding and periodically during the welding operation to incure that both are in compliance with the set requirements. The preheat temperature is to be measured on the surface of the material being welded on the side on which welding is to be performed and within 3" of the area to be welded. The interpass temperature is to be measured on the surface of the material to be welded on the side on which welding is to be performed and within 1" of the weld joint edge and along the joint within 3" of the start of the next weld pass.

The electrodes used for the welding of HY-80 steel are to be conditioned and maintained for issue and use by baking to be followed by storing in holding ovens.

The conditioning by baking is to take place at a temperature of 800°F ± 25°F for a total time at temperature of between 30 minutes and one (1) hour. The oven temperature is not to be in excess of 300°F when the electrodes are placed in the oven for conditioning and the oven temperature is not to be allowed to rise more than 300°F per hour once the oven temperature exceeds 500°F.

Once the electrodes have been conditioned by baking, they are to be transferred to holding ovens while still hot. The transfer to to be accomplished in a sheltered area protected from inclement weather and in such a way as to prevent the temperature of the electrodes from dropping below 150°F. The holding oven temperature is to be in the range of 225°F to 300°F.

Periodic moisture determinations are to be performed after the conditioning baking of the electrodes and upon their removal from the holding ovens and prior to their use. The maximum permissable moisture content of the electrode is 0.20 percent.

During the SMA fusion welding process, the heat input to the HY-80 steel from the welding arc must also be controlled to within a

maximum limit, as determined from the formula:

$$\text{Heat Input (Joules/Inch)} = \frac{\text{Arc Voltage} \times \text{Welding Amperes} \times 60}{\text{Rate of Travel (Inches per Minute)}}$$

Table B-5 gives the maximum values of heat input allowed.

The heat input to the HY-80 steel can be controlled through the control of any of the three variables:

1. Arc Voltage
2. Welding Amperes
3. Rate of Travel

Another means of controlling the heat input is through the control of the weld metal bead length per electrode. The minimum allowable weld metal bead length per electrode for the SMA fusion welding of HY-80 steel is given in Table B-6.

WELDING TECHNIQUE

At the start of the arc, the molten weld metal puddle does not have the full protection of the covered electrode flux coating and porosity of the weld metal can result. To avoid this occurrence, the arc should be struck approximately one inch ahead of the desired starting spot and then rapidly back-stepped. This technique will result in the weld metal deposited at the start of the arc to be remelted as the welding progresses and thus be cleansed of any gases

Thickness	Maximum Joules/Inch
less than 1/2 inch	45,000
1/2 inch and greater	55,000

TABLE B-5: MAXIMUM HEAT INPUT FOR WELDING HY-80 STEEL[12]

Thickness (Inches)	Electrode Size	Minimum Bead Length per Electrode (12 inch Burnoff)
less than 1/2 inch	1/8 in.	4 in.
	5/32 in.	5-3/8 in.
	3/16 in.	8 in.
1/2 inch and greater	1/8 in.	3-3/8 in.
	5/32 in.	4-3/8 in.
	3/16 in.	6-1/4 in.
	7/32 in.	11-3/8 in.

TABLE B-6: MINIMUM ELECTRODE BEAD LENGTH FOR WELDING HY-80 STEEL (12)

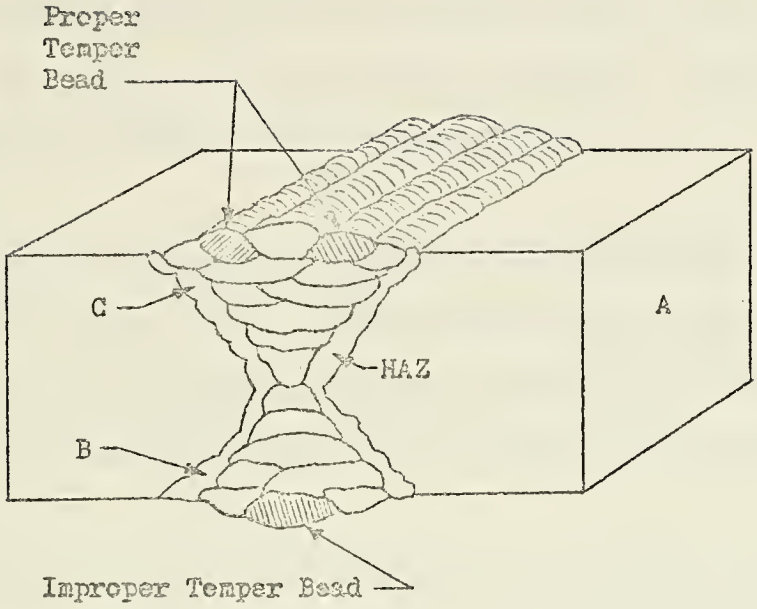

A. Base metal with Brinell Hardness of 216.

B. HAZ of region with proper temper-bead technique and Brinell Hardness of 245.

C. HAZ of region with improper temper-bead technique and Brinell Hardness of 332.

FIGURE B-3: TEMPER-BEAD TECHNIQUE FOR WELDING HY-80 STEEL[12]

or impurities.

During the welding process a drag technique should be used to insure that the arc length is kept as short as possible. Lengthening of the welding arc may result in weld metal proosity.

The stringer-bead technique, and not the weave technique, of weld metal deposit should be used. This technique will result in the most efficient weld progression and thus incure that the maximum limit of heat input and minimum limit of bead length are not violated.

The temper-bead technique should be used in the placing of the finish bead. This technique will result in a tempering of the heat affected zone and thus reduce the brittle condition and the tendency for cracking.

The overlap of the temper-bead must be carefully controlled in order to achieve the desired results. An insufficient overlap of the temper-bead will result in an ineffective temper of the heat affected zone, while an excessive overlap of the temper-bead will result in the creation of a new heat affected zone. The proper overlap of the temper-bead for an effective temper of the heat affected zone required 3/32 inch to 1/8 inch of the outside bead to be exposed between the temper-bead and the heat affected zone. Figure B-3 shows both the proper and improper placement of the temper-bead and the results of each.

APPENDIX C

UNDERWATER WELDING PROCEDURE[29]

FILLET WELDING IN THE HORIZONTAL POSITION

The following is the recommended procedure for fillet welding in the horizontal position:

1. Make sure the safety switch is open.
2. Thoroughly clean the surfaces to be welded.
3. Set the welding generator to deliver the proper current for the electrode being used. This current is higher (0 - 30 percent) than the topside current for the same electrode since the surrounding water absorbs the heat rapidly.
4. Place the striking end of the electrode against the work so that the electrode is at an angle of approximately 30 degrees to the line of weld. This angle may vary from 15 degrees to 45 degrees, depending on the type of electrode used and the personal preferences of the diver.
5. Call for "current on". The arc should start when the tender closes the safety switch. If the arc does not start, tap or scrape the end of the electrode against the work until the arc starts. Once the arc has started, exert sufficient pressure against the work to allow the electrode to consume itself. Maintain the original angle between the electrode and line of weld by moving the hand perpendicularly toward the surface being welded as shown in Figure C-1. Do not hold an arc as in topside welding.

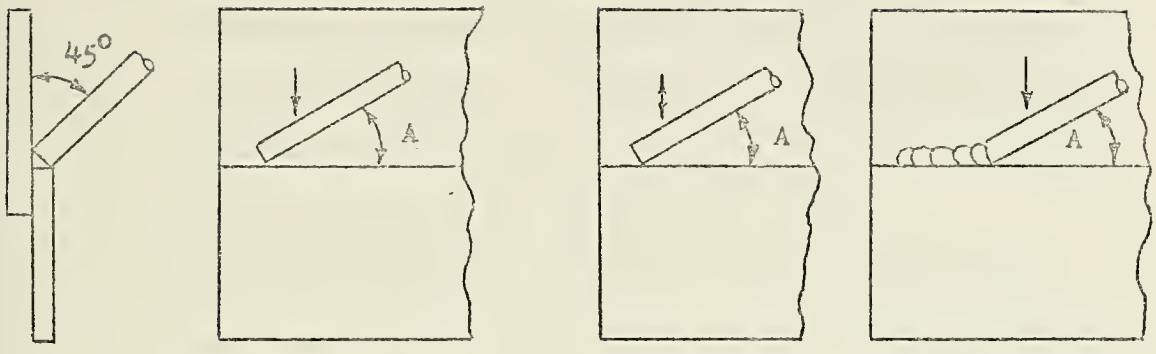

Angle A = $30^{\circ} \pm 15^{\circ}$

a. Position the electrode at an angle of approximately 30 degrees to the line of weld with the electrode tip in contact with the work.

b. Call for current "on". Withdraw electrode momentarily, if necessary, to start the arc.

c. Apply sufficient pressure in the direction of the arrow to allow the electrode to consume itself.

FIGURE C-1: SELF-CONSUMING TECHNIQUE FOR UNDERWATER SHIELDED METAL-ARC WELDING OF HORIZONTAL FILLET WELDS

Simply keep the electrode in contact with the work, maintaining the original angle between the work and the electrode. Run straight beads, do not weave. About 8 inches of weld metal is deposited for every 10 inches of electrode consumed. This method is a definite advantage especially where poor visibility would make it difficult to hold an arc in the usual topside manner.

6. When the electrode is consumed call for "current off". The tender must open the safety switch and keep it open while the diver is changing electrodes. Keep the electrode in welding position after completing the weld until verification of "current off" is received from the tender.

7. Before starting to deposit a new electrode, clean the end of the previous deposit. The deposit from the new electrode should slightly overlap the previous deposit. If a second pass is to be added, the entire previously deposited weld must be thoroughly cleaned.

8. Do not call for "current on" until the new electrode is in position against the work and ready for welding. In general, weld so that the bubbles generated interfere with the visibility as little as possible. For example, it is usually better for the diver to weld toward rather than away from himself.

FILLET WELDING IN THE VERTICAL POSITION

The same technique should be used for fillet welding in the vertical position as that recommended for horizontal fillet welds. Vertical fillet welds should be made from the top down as shown in Figure C-2. In this way the bubbles generated do not interfere with the diver's visibility in following his line of weld. Depending on individual conditions, a slight variation of the electrode to work angle and the current selected for horizontal work may prove advantageous.

FILLET WELDING IN THE OVERHEAD POSITION

The "self-consuming" technique can be applied to fillet welding in the overhead position (Figure C-3) when using the approved electrodes designated, provided the current is carefully adjusted. The current range for overhead welding is very narrow. Welds deposited using current rates outside this range will result in very poor deposits or no deposit at all. Good penetration and fusion can be obtained readily but undercutting and convex beads are difficult to avoid with this technique.

An alternate technique for overhead welding, requiring greater skill, involves the use of an angle of approximately 35° - 55° between the electrode and line of weld and a slow, steady rate

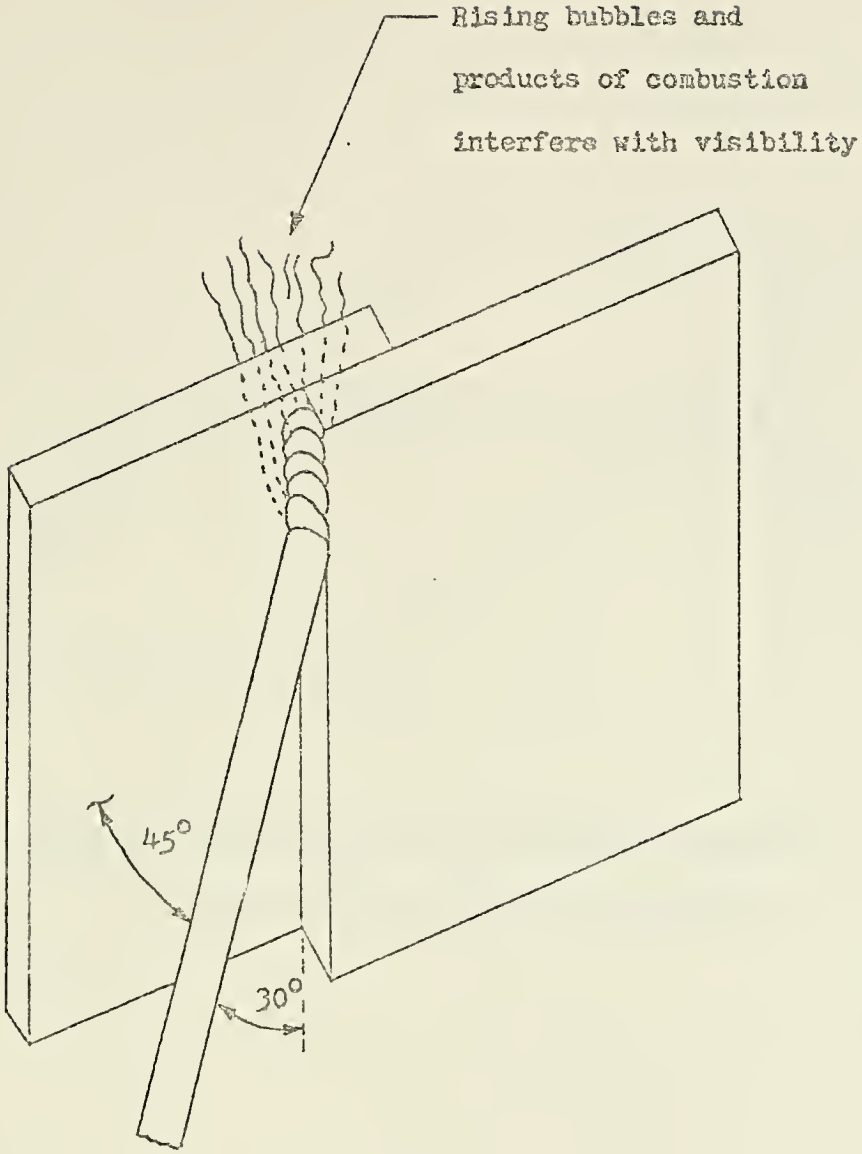

FIGURE C-2: SELF-CONSUMING TECHNIQUE FOR UNDERWATER SHIELDED METAL-ARC WELDING OF VERTICAL FILLET WELDS

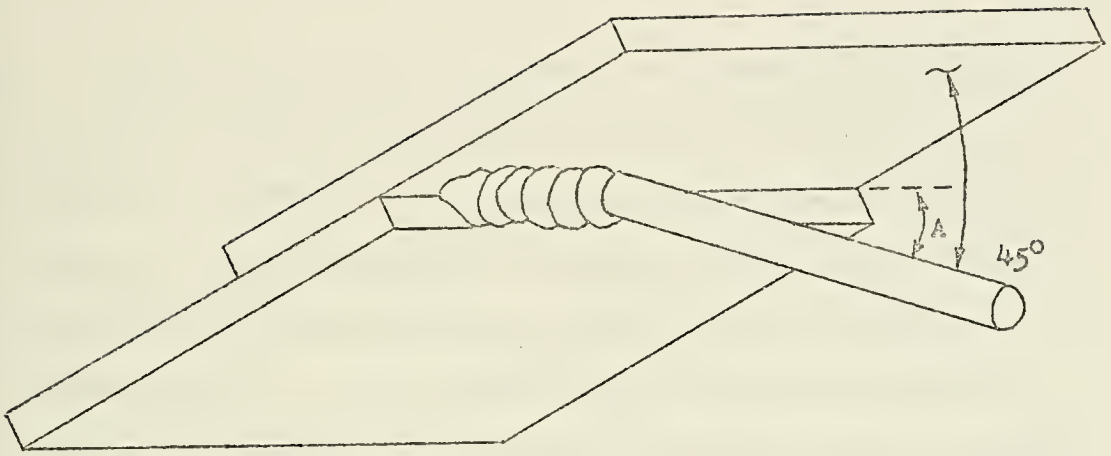

Angle A = 15° to 45° for self consuming technique

35° to 55° for "35° - 55°" technique

FIGURE C-3: TECHNIQUE FOR UNDERWATER SHIELDED METAL-ARC WELDING OF OVERHEAD FILLET WELDS

of progression governed by the diver-welder. With practice, overhead welds employing this 35° - 55° technique can be produced with the convexity and undercutting which is obtained when using the "self-consuming" technique.

The "self-consuming" technique is recommended for operators of average or less than average skill who have little time for practice. The "35° - 55°" technique is recommended for skilled operators. Before attempting an actual overhead weld by either technique, the diver should make several practice runs under working conditions. These welds should be brought topside and examined to ascertain that the current setting is correct and that the diver has mastered the technique. Dripping beads indicate that (1) the current was too high, (2) the operator applied insufficient pressure, or (3) that there existed a combination of both. Skill, coupled with practice, is essential to the production of consistently good overhead welds.

APPENDIX D

EXPERIMENTAL UNDERWATER WELDING OF HY-80 STEEL

BACKGROUND

A series of three working dives were performed at the Naval School - Diving and Salvage, Washington Navy Yard, Washington, D.C., in accordance with United States Navy regulations governing underwater welding operations as outlined in Navships 0929-000-8010.

All three of the dives were carried out wearing a Navy Standard MKV hard hat diving system, in fresh water, at a depth of twelve (12) feet, at a water temperature of 71°F (21.7°C), in the open tanks of the Naval School - Diving and Salvage facility.

The intent of these working dives was to extend the laboratory work of Meloney[22] to a practical application that simulated the repair of a crack in the underwater body of a vessel, as is described in Navships 0929-000-8010. This provided an opportunity to perform the underwater welding of HY-80 steel in the verticle and overhead as well as downhand position and to evaluate the effect of bubble generation, turbidity, visibility, and limited mobility on the working diver's ability to produce the desired welds.

EQUIPMENT

All of the equipment used for the three working dives was in accordance with the specifications of Navships 0929-000-8010.

Power supply. A direct-current welding generator with an ampere capacity range of from 120 amperes to 750 amperes was used. The welding generator was connected for direct-current straight polarity operation as is shown in the schematic diagram in Figure D-1.

Safety switch. A positive-acting disconnecting safety switch was installed in the welding electrical circuit as is shown in the schematic diagram in Figure D-1. This safety switch was of the type that is currently supplied for underwater welding and cutting operations and is specified as follows:

Knife Switch

Type K, Infusible

Single Pole, Single Throw

300 Amperes, 250 Volts

This safety switch was kept open at all times, except when the diver had the electrode in position for welding and had directed the diving tender to close the safety switch. This afforded the diver the maximum protection possible by having the electric current on only when the welding operation was actually taking place.

Cable. Size 2/0 (133,000 circular mils) extra flexible welding cable conforming to Military Specification MIL-C-915, Type TRXF was used for connecting the power supply to the safety switch and the safety switch to the leader attached to the electrode holder. The

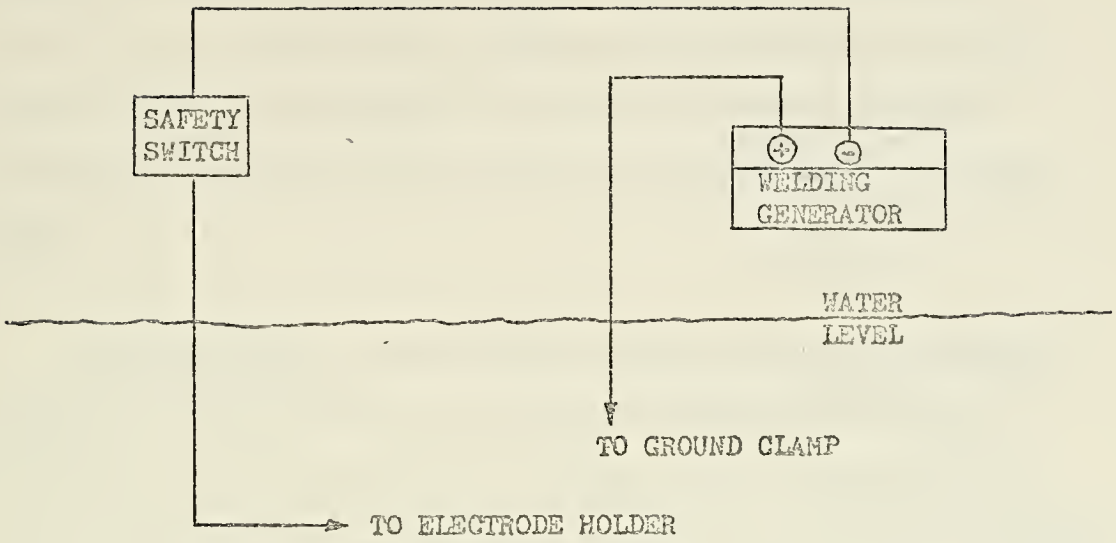

FIGURE D-1: SCHEMATIC DIAGRAM OF THE UNDERWATER WELDING EQUIPMENT ARRANGEMENT FOR THE DIRECT-CURRENT STRAIGHT POLARITY UNDERWATER WELDING OF HY-80 STEEL

leader attached to the electrode holder was a size 1/0 (105,000 circular mils) extra flexible welding cable conforming to Military Specification MIL-C-915, Type TRXF, and was ten feet in length. This leader was used to aid the diver in maneuvering the electrode holder.

Electrode holder. The electrode holder used was a recommended underwater electrode holder conforming to Military Specification MIL-H-865, Type MIL-300, Class 1, Buships Dwg. No. S-9400-921592. This electrode holder was completely insulated and provided protection for the diver from the bare grip end of the electrode.

Accessories. A supplementary welding lens face plate incorporating a spring-loaded, fluted washer, face-plate positioning device which fitted the MKV diving helmet and held a No. 6 welding glass conforming to Buships Dwg. No. S9400-921592, was used. This assembly provided the maximum protection possible to the divers eyes from the flash of the welding arc.

The additional accessory materials that were used consisted of a grounding clamp and a wire brush and scraper for cleaning the base metal and removing slag from the weld metal.

MATERIALS

The consumable materials required for the underwater SMA fusion welding consisted of 1/8 in. E-11018 iron powder electrodes, parafin wax waterproofing material, and 1/4 inch HY-80 steel plate conforming to Military Specification MIL-S-16216.

PREPARATION

The welding parameters for the underwater welding of 1/4 inch HY-80 steel plate, experimentally determined by Maloney[22] and shown in Table D-1, were used as a basis for determining the proper welding generator settings. After producing a series of practice welds at different settings, it was found that the particular welding generator being used and the working conditions yeilded the best welds with a setting of 190 amperes/32 volts for the downhand position and a setting of 120 amperes/32 volts for the vertical and overhead positions.

The flux of the E-11018 iron powder covered electrodes was impregnated with the parafin wax by rubbing a block of the water-proofing material over the flux coating. After the flux was thoroughly impregnated, the bare-grip end of each electrode was thoroughly cleaned to insure good electrical contact between the electrode and the electrode holder. The tip of each electrode was also

	E-11018 Low Hydrogen Covered Electrode
	Welding Parameter
Current	180-210 Ampere
Voltage	28-36 Volts
Travel Speed	9.8-12.1 Inches/Minute
Heat Input	32,130-36,020 Joules/Inch
Ambient Temperature	43.6°F

TABLE D-1: EXPERIMENTALLY DETERMINED WELDING PARAMETERS FOR THE UNDERWATER WELDING OF HY-80 STEEL (22)

thoroughly cleaned to insure exposure of the bare core for easy starting of the welding arc.

HY-80 steel plate, 1/4 inch thick, was cut into pieces 8 inches by 6 inches to serve as the underwater body in need of repair, and pieces 4 inches by 3 inches to serve as the doubler plate for the repair. All of the cuts were made by a power hack-saw so that all of the cuts would yeild finished edges.

The mill scale was left on the surface of the HY-80 steel plates. This was done to simulate the paint, rust, and other impurities that would exist on the underwater body in need of repair and could not be removed with the hand tools readily available to the diver under working conditions.

TECHNIQUE

The multi-pass, "self-consuming" stringer-bead technique was used for the downhand, vertical, and overhead underwater welding of the HY-80 steel plate. This decision was made after considering both the advantages and disadvantages of the single-pass and multi-pass methods.

Meloney[22] found that when the single-pass method was utilized, the grain size of the heat affected zone was smaller than the grain

size of both the base metal and the weld metal. The weld metal was also found to contain large dentritic grains with heavy grain boundaries, severe porosity, and microcracks. On the other hand, Meloney[22] found that when the multi-pass method was utilized, although the grain size of the heat affected zone was essentially the same as when the single-pass method was utilized, there was a reduction in the hardness of the heat affected zone due to the tempering affect of the subsequent passes. The weld metal was also found to have no dentritic grains, except in the final pass which had fewer heavy grain boundaries, less porosity, and less microcracking.

The adverse effects of undercut, an unavoidable phenomena of underwater welding, was minimized by utilizing the multi-pass method. This method enabled the diver to "push" the undercut region away from the critical region of the joint and out into the base metal.

The fillet lap joint of the doubler plate configuration was conducive to the use of the multi-pass method. The groove created by the edge of the doubler plate and the surface of the underwater body plate provided a guide for the positioning of the electrode.

PROCEDURE

The actual procedure followed in the underwater welding of the

HY-80 steel doubler plates was in accordance with Navship 0929-000-8010, as is described in Appendix C.

The welding sequence followed in utilizing the multi-pass, "self-consuming", stringer-bead technique is shown in Figure D-2.

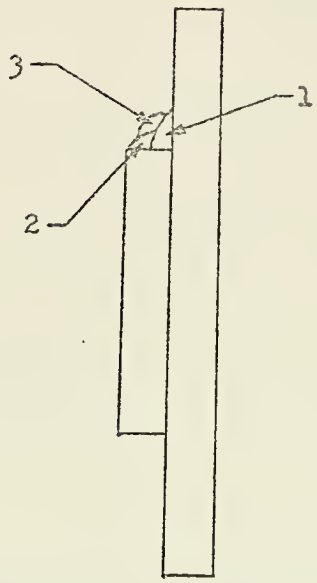

FIGURE D-2: WELDING SEQUENCE FOLLOWED FOR THE UNDERWATER WELDING OF 1/4 INCH HY-80 STEEL DOUBLER PLATES

PART V

REFERENCES

1. Baker, R.G., Watkinson, F., and Newman, R.P., "The Metalurgical Implications of Welding Practice as Related to Low Alloy Steels", Significance of Defects in Welds, Proceedings of First Conference, February 23-24, 1967, London, England.

2. Boniszewski, T., Watkinson, F., and Baker, R.G., "Heat Effected Zone Cold Cracking of Low Alloy Steels", Significance of Defects in Welds, Proceedings of First Conference, February 23-24, 1967, London, England.

3. Brick, R.M., Gordon, R.B., and Phillips, A., Structures and Properties of Alloys, Third Edition, McGraw-Hill, 1965.

4. Brown, A.J., Brown, R.T., and Masubuchi, K., "Interum Report on Fundamental Research of Underwater Welding", M.I.T., February, 1973.

5. Brown, A.J., Staub, J.A., and Masubuchi, K., "Fundamental Study of Underwater Welding", Offshore Technology Conference #1621, 1972, Houston, Texas.

6. Brown, R.T., "Considerations in Underwater Multi-pass Welding" Proposal on Investigation of Underwater Welding Procedures in Producing Optimum Joint Mechanical Properties, Department of Ocean Engineering, M.I.T., March 13, 1972.

7. Burdekin, F.M., Harrison, J.D., and Young, T.G., "The Effect of Weld Defects with Special Reference to BWRA Research", Significance of Defects in Welds, Proceedings of First Conference, February 23-24, 1967, London, England.

8. Cabelka, J. "Delayed Cracks in Welded Joint", Proceedings of the First International Symposium: Cracking and Fracture in Welds, November, 1971, Tokyo, Japan.

9. Clark, D.S., and Varney, W.R., Physical Metallurgy for Engineers, Second Edition, American Book Company, 1962.

10. Coe, F.R., "The Avoidance of Hydrogen Cracking in Welding", Proceedings of the First International Symposium: Cracking and Fracture in Welds, November, 1971, Tokyo, Japan.

11. Cotterill, P., The Hydrogen Embrittlement of Metals, Pergamon Press, 1961.

12. Fabrication, Welding, and Inspection of HY-80 Submarine Hulls, Navships 0900-006-9010, Bureau of Ships, Navy Department, Washington, D.C., June, 1966.

13. Flax, R.W., Keith, R.E., and Randall, M.D., Welding the HY Steels, ASTM Technical Publication 494, #04-494000-02, American Society for Testing and Materials, 1971, Philadelphia, Pennsylvania.

14. Fujita, Y. and Nomoto, F., "Studies of Thermal Stresses in Welding with Special Reference to Weld Cracking", Proceedings of the First International Symposium: Cracking and Fracture in Welds, November, 1971, Tokyo, Japan.

15. Crubbs, C.E. and Teth, O.W., "Multi-pass All Position 'Wet' Welding - A New Underwater Tool" Offshore Technology Conference #1620, 1972, Houston, Texas.

16. Holt, D., "The Influence of Weld Defects on Service Performance", Significance of Defects in Welds, Proceedings of First Conference, February 23-24, 1967, London, England.

17. Kikuya, Y. and Araki, T., "A Fundamental Research on the Diffusivity of Hydrogen in Steel and its Effect on the Embrittlement and Delayed Failure of Steel", Proceedings of the First International Symposium: Cracking and Fracture in Welds, November, 1971, Tokyo, Japan.

18. Kobayashi, T. and Aoshima, T., "Welding Cracks in Low Alloy Steels", Proceedings of the First International Symposium: Cracking and Fracture in Welds, November, 1971, Tokyo, Japan.

19. Masubuchi, K., "A Condensed Report on Underwater Cutting and Welding State-of-the-Art", Materials for Ocean Engineering, M.I.T. Press, May, 1970.

20. Masubuchi, K., Text for 13.17J, Welding Engineering, M.I.T., December, 1973.

21. Masubuchi, K., and Martin, D.C., "Mechanisms of Cracking in HY-80 Steel Weldments", AWS 43rd Annual Meeting, Cleveland, Ohio, April 9-13, 1962.

22. Meloney, M.B., "The Properties of Underwater Welded Mild Steel and High Strength Steel Joints", OE and SM(NAME) Thesis, M.I.T., June, 1973.

23. Pluger, A.R., Lewis, R.E., and Willner, E., "Review of American Thinking on the Problem of Weld Imperfections", Significance of Defects in Welds, Proceedings of First Conference, February 23-24, 1967, London, England.

24. Reed-Hill, R.E., Physical Metallurgy Principles, Van Nostrand, New Jersey, 1964.

25. Rothman, R.L, and Monroe, R.E., "Underwater Welding Evaluation", Battelle Columbus Laboratory, Columbus, Ohio, July 26, 1973.

26. Savage, W.F., "What is a Weld?" Rensselear Polytechnic Institute, Troy, New York.

27. Standard Handbook for Mechanical Engineers, Seventh Edition, McGraw-Hill, New York, 1967.

28. Ueda, Y., and Yamakawa, F., "Mechanical Characteristics of Cracking of Welded Joints", Proceedings of the First International Symposium: Cracking and Fracture in Welds, November, 1971, Tokyo, Japan.

29. Underwater Cutting and Welding Technical Manual, Navships 0929-000-8010, U.S. Navy Supervisor of Salvage, Naval Ships Systems Command, Washington, D.C., November, 1969.

30. U.S. Papers for Japan - U.S. Seminar, Significance of Defects in Welded Structures, Tokyo, Japan, October 16-19, 1973.

31. Weldability of Steels, Welding Research Council, New York, New York, 1971.

32. Willi, A., and Baach, H., "Water Content in Submerged-Arc Fluxes and its Influence Upon Weld Cracking", Proceedings of the First International Symposium: Cracking and Fracture in Welds, November, 1971, Tokyo, Japan.

Thesis
R338 Renneker
An investigation of underwater welded HY-80 steel.